IMPERIAL COLLEGE LONDON

Department of Earth Science and Engineering

Centre for Petroleum Studies

A Novel Computational Approach to Obtain Contact Angles:
Application to Carbon Capture and Storage

By

Manu Savio Mathew

A report submitted in partial fulfilment of the requirements for the MSc and/or the DIC.

September 2011

Declaration of Own Work

I declare that this thesis **"A Novel Computational Approach to Obtain Contact Angles: Application to Carbon Capture and Storage"** is entirely my own work and that where any material could be construed as the work of others, it is fully cited and referenced, and/or with appropriate acknowledgement given.

Signature:.....

Name of student: Mr. Manu Savio Mathew

Name of supervisor: Dr.Fernando Bresme
Dr. Stefan Iglauer

Acknowledgements

I would like to express my sincere gratitude to my supervisors, Dr. Fernando Bresme and Dr. Stefan Iglauer. This project is an outcome of their exceptional mentoring and support they offered me during the course of the project.

I would also like to thank Dr.Frank Romer, Serapian Stefano, Wendy Zhang, Sebastian Kutsch and Jordan Muscatello for spending their invaluable time with me to guide the project in the right path. I appreciate the effort they have put in, to solve the problems encountered during the project.

I am greatly debted to my friends and family for their prayers and encouragement during the difficult times of the course.

Last but not the least; I would like to offer my appreciation to the Imperial College authorities for considering me worthy to do this project and for providing the necessary technical support.

Table of Contents

Table of Figures

List of Tables

Imperial College
London

A Novel Computational Approach to Obtain Contact Angles: Application to Carbon Capture and Storage

Manu Savio Mathew

Imperial College supervisor – Fernando Bresme and Stefan Iglauer

Abstract

Climatic changes due to the emission of excess CO_2 into the atmosphere are a serious threat. Carbon Capture and Storage (CCS) projects are thus becoming important to fossil fuel burning power stations as several jurisdictions have been employed on the amount of CO_2 that can be emitted into the atmosphere. But one essential problem faced by the power stations is to estimate the amount of CO_2 that can be stored in the geological formations safely. One main uncertainty behind such projects is the interfacial interactions between the reservoir rocks-water-CO_2. Interfacial interactions can be quanitified through interfacial tensions and contact angles. Hence, an accurate prediction of interfacial tension and contact angle can reduce uncertainty and risk.

Currently, the interfacial interactions are evaluated using a limited number of experimental results; however these results are partially contradicting each other. Moreover, these experimental results do not represent the wide range of reservoir conditions that exist in the field.

In this work, a computational model is developed to give microscopic insights on the interfacial interactions including interfacial tension and wettability of a carbon dioxide-water-quartz (CO_2-H_2O-SiO_2) system. Molecular dynamics simulations were performed which can predict the interfacial tension and contact angles of a typical CO_2-H_2O-SiO_2 system using the DL_POLY code. The study focused on the effect of variation of temperature, pressure and salinity on the interfacial tension and hence the contact angle of a water droplet on a quartz surface (surrounded by CO_2). It was found that the TIP4P-2005 water model and EPM2 better reproduced the the experimental values of interfacial tension between CO_2 and water than previous simulation models. The simulations to obtain the contact angles for various thermodynamic conditions suggest that the contact angle is influenced to a greater extent by the CO_2-quartz and salt-quartz interfacial interactions than the CO_2-brine interactions.

Introduction

Carbon Capture and Storage (CCS) is a technology to mitigate climatic changes by storing CO_2 deep inside geological formations (IPCC 2005). CO_2 can be stored in deep saline aquifers, unminable coal seams and depleted oil or gas reservoirs. There are four ways of trapping the CO_2 namely stratigraphic or structural trapping, dissolution trapping, mineral trapping and capillary trapping. The project focuses on capillary trapping which occurs when injected CO_2 is trapped inside the pores of rock by water (Juanes et al. 2006). It is also related to structural trapping capacities (IPCC 2005).

The main factors influencing the amount of CO_2 stored in the pores are interfacial tensions and contact angles (Spiteri et al. 2008). CO_2 can break through the cap rock if stored above the CO_2 break-through pressure (Naylor et al. 2011). Currently, there are no efficient technologies which can counter such cap rock leakages. So an accurate measurement and prediction of contact angle and interfacial tensions are necessary to predict potential leakage, estimate residual trapping and improve risk and capacity assessments. Moreover, such experimental works are expensive and time consuming; so there is a need to rapidly and accurately predict the contact angles for a CO_2-H_2O-SiO_2 system.

A number of experimental works were completed in the past to describe the relationship of contact angles and interfacial tension with pressure, temperature and salinity conditions; however the results for quartz surfaces are inconclusive. Dickson et al. (2006), measured the contact angles of CO_2/water/glass. Two different glass substrates were used with silicon hydroxide (SiOH) coverages of 12% and 37% (with the remainder being methylated). The contact angle increased with pressure for both substrates but the change was more pronounced (98^o-148^o) for the substrate with less hydrophilic nature (12% SiOH). Yang et al. (2008) used axisymmetric drop shape analysis techniques to investigate the contact angle of reservoir brine –reservoir rock system with dissolution of CO_2 at high pressures and elevated temperatures. According to their experiment, the equilibrium contact angle increases with pressure and decreases with temperature. Dickson et al. (2006) and Yang et al.'s (2008) substrates were CO_2 wet as contact angles were greater than 90^o. It should be noted that although contact angle values can give a rough indication of CO_2 wettability, they cannot be directly used to draw conclusions for reservoir rocks as the contact angle measurements are performed on an idealized surface area.

Chiquet at al. (2007) measured contact angles on quartz and mica with the captive drop techniques and CO_2 wetting of caprock was found to increase with CO_2 pressure. Espinoza and Santamarina (2010) extended the scope of previous studies to other substrates including quartz, calcite, oil wet quartz, polytetrafluoroethylene (PTFE) and pore fluid conditions that are similar to those in geological formations. They found that the contact angle increases on non wetting surfaces such as PTFE and oil wet quartz and decreases in case of water-wet and calcite surfaces. These results contradict the work of Chiquet et al.

(2007) and Yang et al. (2008). Bikkina (2011) investigated the influence of drop volume, pressure, temperature and repeated exposure of quartz and calcite surfaces to dense water saturated with CO_2 on contact angle and found that the contact angle was significantly altered by the presence of water saturated CO_2. But his studies do not consider the presence of salt which is typically found in a deep saline aquifer.

Chalbaud et al. (2009) conducted pore scale wettability studies for glass micromodels of different hydrophilicities. The work indicates that the CO_2 does not wet the solid surface in the case of a strongly hydrophilic porous media but if the porous surface is less hydrophilic, the CO_2 wets the surface. In a capillary pressure experiment Plug and Bruining (2007) found that clean quartz sand can be CO_2-wet during waterflooding.

The first molecular dynamics simulations of wetting behavior at CO_2/water/solid interfaces were performed by Liu et al. (2010). They concluded that contact angle of the water droplet on the hydrophilic surface increases with fluid density (but no separation of water droplet is observed from the surface at high CO_2 pressures), whereas water would detach from hydrophobic surfaces upon a small increase in the CO_2 density. The authors did not consider in this model the influence of salinity or temperature on the contact angle.

In this paper, the information from the above experimental and simulation works are used to develop an accurate computational model to predict the variation of water-CO_2-SiO_2 contact angle for thermodynamic conditions characteristic of reservoirs including salt effects and pressure and temperature changes.

Molecular Dynamics Simulation

Molecular dynamics is a computer simulation method that can be used to investigate the structure and motion of atoms, molecules or molecular assemblies using microscopic information based on intermolecular potentials. In most cases, the motion of the interacting molecules is tracked by solving the Newton's equation of motion. The forces between the particles and the potential energy are defined using force fields (Alder et al. 1959, Leach 2001). These force fields are derived from experimental measurements and quantum mechanical computations. In this work, a molecular dynamics code called DL_POLY is used (Smith et. al. 2008).

Simulation Model and Design

The potential model of water used here is the TIP4P-2005 model (Abascal and Vega 2005). The EPM2 model was used for the CO_2 simulation (Harris and Yung 1995). In these models, the intermolecular interaction is taken into account using the Lennard Jones and the Coulomb potentials. The alpha quartz surface used in the presented simulations is a Si-O-Si bridged surface (Figure 1). From an orthorhombic unit cell, a periodically repeating supercell was created to model an alpha quartz slab. The force field parameters are listed in Table 1 below. The interatomic potential used in the silica simulation is of the form given by (Krammer et al. 1990).

$$\emptyset_{ij} = \frac{q_i \times q_j}{r_{ij}} + A_{ij} \times e^{(-b_{ij} \times r_{ij})} - \frac{C_{ij}}{r_{ij}^6} \quad (1)$$

where,

$\emptyset_{ij}$= interaction energy of atoms i and j,
q= site charge,
A= short range parameter (cluster parameter),
C= bulk parameter,
b= repulsion exponent,
$r_{i,j}$= distance between i and j atoms,
e = electron charge.

Table 1: Force field parameters of silica

i-j	Short Range Parameters		C_{ij} {(kJ/mol) (nm^6)}	Atomic Charges (q/e)
	A_{ij}(kJ/mol)	b_{ij}x10 $(nm)^{-1}$		
O-O	133,920	2.76	0.01688	-1.2
Si-O	1,737,102	4.87	0.01288	2.4

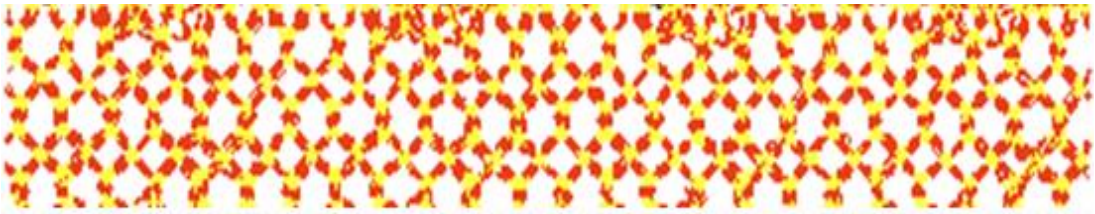

Figure 1: Silica structure used in the simulations (Red-Silicon, Yellow-Oxygen)

The Lorentz Berthelot (equation 2 and 3 below) mixing rules (Allen et al. 1989) were used to treat the interaction between unlike particles. The long range Coulombic interaction was treated using the Ewald summation method (DL_POLY/2.19 2008). All the simulations were run using periodic boundary conditions. Most of the simulations were run for 50,000 steps to equilibriate the system with a timestep of 0.002 picoseconds (ps) and 10^6 production steps except for the CO_2-water simulations. For the CO_2-water system, a total of 500,000 production steps were run. 1.7 nm was used as the cut off for the Van der Waals (vdW) interactions for the production runs using the CO_2-water model and SiO_2- CO_2-water model. This means that when the distance between 2 atoms exceeds 17Å the van der Waals forces are set to zero, although the atoms interact through the long-range Coulomb forces at all distances.

$$\varepsilon_{ij} = \sqrt{\varepsilon_i \times \varepsilon_j} \tag{2}$$

$$\sigma_{ij} = \frac{(\sigma_i + \sigma_j)}{2} \tag{3}$$

where,

ε=depth of potential well,

σ=collision diameter.

The works performed in this study are outlined below:-

First Phase:-

- The TIP4P-2005 water model was validated against the experimental values of water density at various temperatures ranging from 250K-350K and 1bar pressure.
- Simulations were carried out using the CO_2 model. The density values obtained from the simulations were then validated against experimental values of CO_2 density.
- The CO_2-water model obtained after merging the TIP4P-2005 model and CO_2 model was then used to compute the interfacial tensions at pressures ranging from 1MPa-20MPa. Results were compared with experimental values.
- Simulations were done on the CO_2-brine model to see the effect of salt on IFT.

Second Phase:-

- Simulations were run to obtain contact angles of SiO_2-water-CO_2 systems for various pressure, temperature and salinity conditions. Results were compared with experimental values.
- Few simulations were run using the SiO_2-brine-CO_2 model to see the effect of salt on contact angle.

Validation of the TIP4P-2005 Water Model: As a first step, simulations were run using the potential TIP4P-2005 water model for various temperatures ranging from 275K-300K at a constant pressure of 1bar. The starting simulation cell size was 1.966nm x 1.966nm x 1.966nm. All simulations were run in the isothermal-isobaric (NPT- number of particles, temperature and pressure are kept constant) ensemble (DL_POLY/2.19 2008). 256 water molecules were used for the simulation; these were found to be adequate for the molecular dynamics simulation of the TIP4P-2005 model (Abascal& Vega 2005). The cutoff for Van der Waal's interactions was set to 0.9nm which has been shown to represent molecular interactions adequately (Abascal & Vega 2005). The smaller vdW cutoff was used because the cell width of this system was small compared to the other systems used for production runs. Generally, a cutoff value less than half the cell width should be used or else it can result in the computation of interactions of one particle with its image. The Lennard Jones potential model is used for the interaction between oxygen atoms with the depth of potential well, ε =0.775kJ/mol and diameter, σ=0.316nm. Simulation results were highly consistent with experimental results (Figure 2).

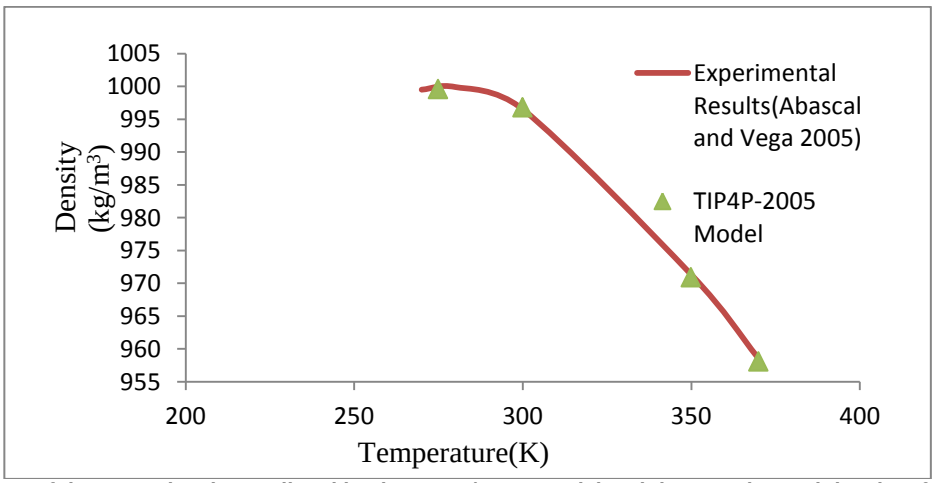

Figure 2: Comparison of the water density predicted by the TIP4P/water model and the experimental density of water (Abascal and Vega 2005) at 0.1MPa pressure.

Validation of the EPM2 CO_2 Model: Simulation using the EPM2 model was carried out for temperatures ranging from 220K – 280K at 7.1MPa pressure.The starting box dimension of the simulation was 2.48nm x 2.48nm x 2.48nm. Simulations were run in NPT ensemble.The vdW cutoff was set to 0.9nm.This is because the vdW cutoffs should be shorter than half the cell width. 216 CO_2 molecules were used for this simulation. From the Figure 3 below, it is very clear that the model slightly underpredicts the liquid coexistence densities between the temperature ranges of 220K-280K. This underprediction of densities is due to the short vdW cutoff used in these simulations.

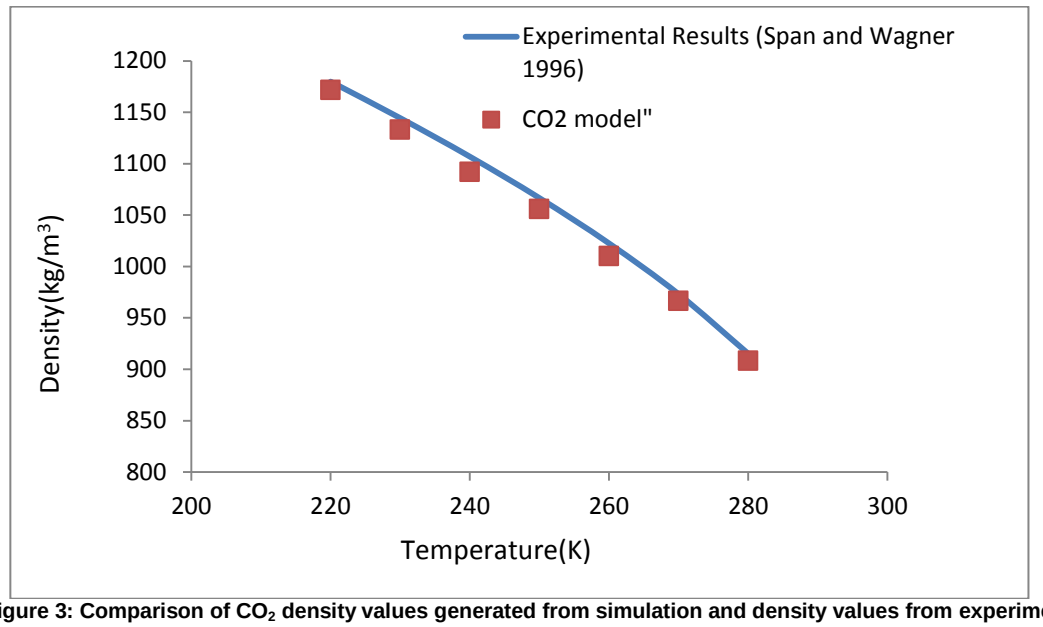

Figure 3: Comparison of CO_2 density values generated from simulation and density values from experiments (7.1MPa).

CO_2-Water Model Simulation: The TIP4P-2005 water and CO_2 models were used to compute the interfacial tension as a function of CO_2 pressure. The simulation box consists of 3 regions with a water slab in the middle surrounded by CO_2 fluid slabs on either side. The simulation box has a dimension of 5.661nm x 5.661nm x 10.553nm in the X, Y and Z directions. The simulations were performed in the canonical ensemble (NVT) which means that the number of particles, volume and temperature of the system is set constant. Simulations of 20000 steps were found to be sufficient to equilibriate the system. The total simulation consisted of 80000 steps. Simulations were run at 300K but for different pressures by varying the number of CO_2 molecules in the simulation box. A total of 5832 water molecules were used for each simulation. The number of CO_2 molecules used in each simulation is given in Table D1 in the Appendix. The Lennard Jones potential parameters are listed in Table C1 in the Appendix.

The CO_2 pressure was computed from the component normal to the CO_2-water interface. This value is then corrected by discounting the Van der Waal's long range corrections, which is added by default in the DL_POLY code. The interfacial tension is then calculated using the equations 4 and 5 given below. The resulting interfacial tension computed is the sum of the two identical interfaces between CO_2 and water that is used in the simulation. So the half of the interfacial tension computed gives the tension of the CO_2-water interface.

$$P_{actual} = P_{zz} - P_{correction} \quad (4)$$

$$\gamma = 0.5 \times \{P_{ZZ} - (P_{XX} + P_{YY}) \times 0.5\} \times L_{ZZ} \quad (5)$$

where,

Pzz, Pyy and Pxx are pressure components of the simulation box in Z, Y and X direction,
$P_{correction}$ is the Van der Waal's correction factor,
Lzz is the box length in the Z direction,
γ is the interfacial tension.

Figure 4 shows that the interfacial tension drops rapidly till it reaches a pressure of 75 bars and then stays approximately constant. This transition from rapid change to constant values can be attributed to the phase change of CO_2 from vapour phase to supercritical (or liquid) phase. This simulation model correlates better with the experimental results of Hebach et al.(2002) and Chun–Wilkinson(1995) than the simulation work of Zhang et al. (2011), especially at low pressures. The model slightly over predicts the interfacial tension values at high pressures (above 7.4MPa) but the interfacial tension trend shown by experimental values are reproduced. This over prediction of IFT is a result of the under prediction of CO_2 solubility by the model when CO_2 changes liquid phase. This model can be improved by increasing the interaction between CO_2 and water.

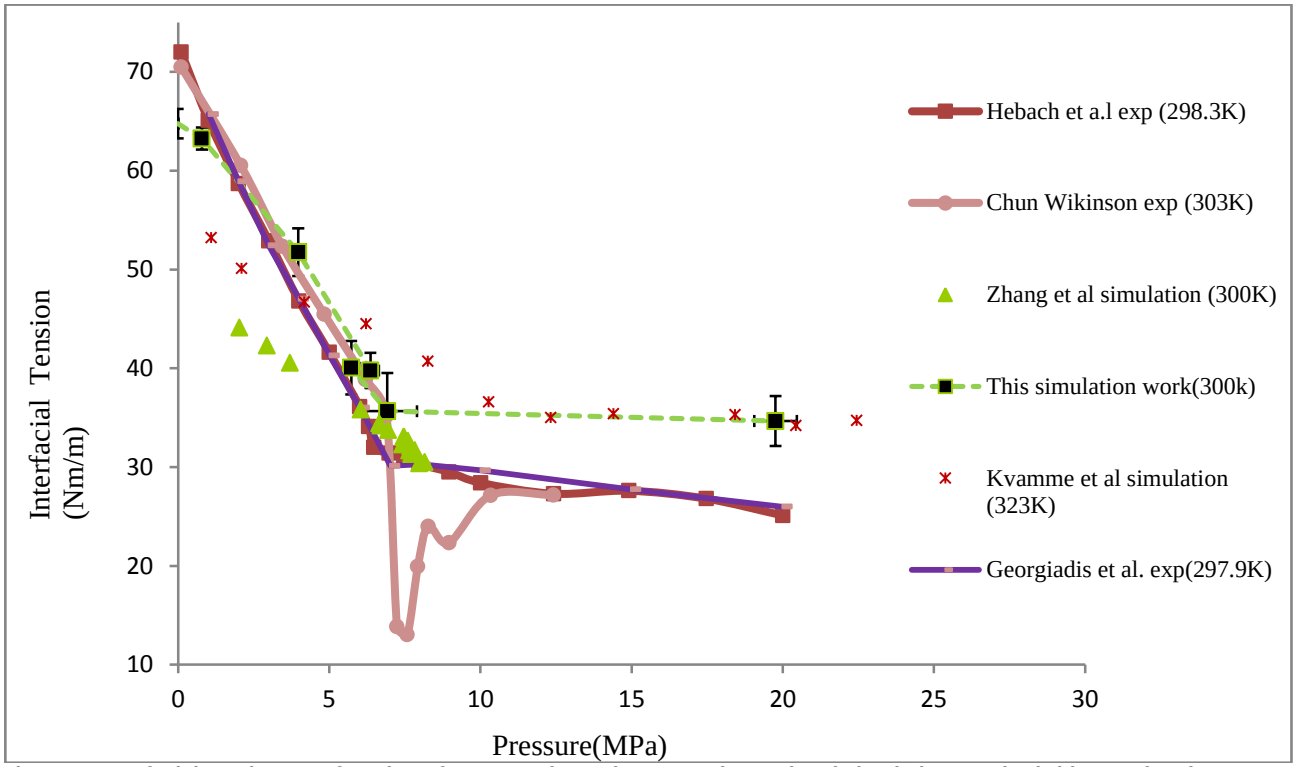

Figure 4: Interfacial tension as a function of pressure for various experimental and simulation results (with error bars).

The computed values of CO_2 densities in the bulk region (Figure5), correlate better with the semi–empirical values of CO_2 density calculated using the equation of states (Span and Wagner 1996) than the simulation model of Zhang et al. (2011).

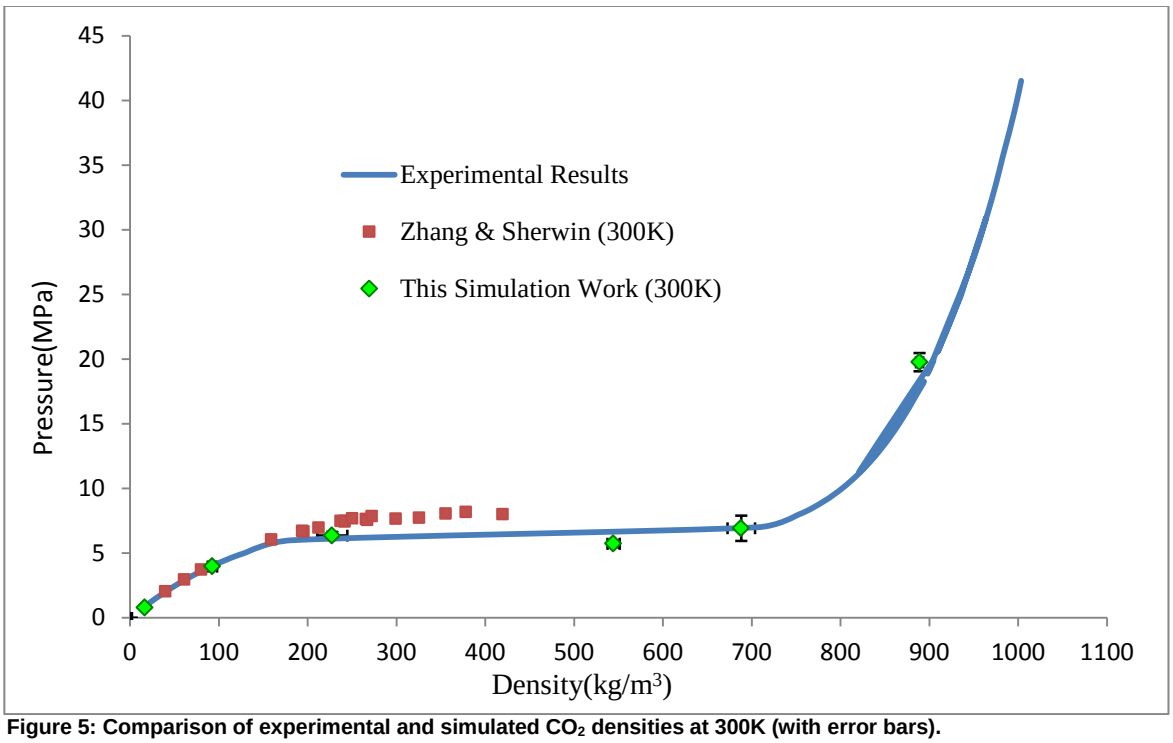

Figure 5: Comparison of experimental and simulated CO_2 densities at 300K (with error bars).

In Figure 6, the bulk water densities stays constant as water compressibility is low. The data A, B, C, D, E, F and G correspond to CO_2 pressures of 20.22MPa, 7.36MPa, 5.8MPa, 6.13MPa, 3.94MPa, .85MPa and 0MPa respectively. It is clear from Figure 6 that increasing the number of CO_2 molecules results in the increase in the bulk CO_2 density and hence increased pressure is applied on the water slab. Note that the density values of curve G are multiplied by a factor of 75 in order to visualize the small density profile.

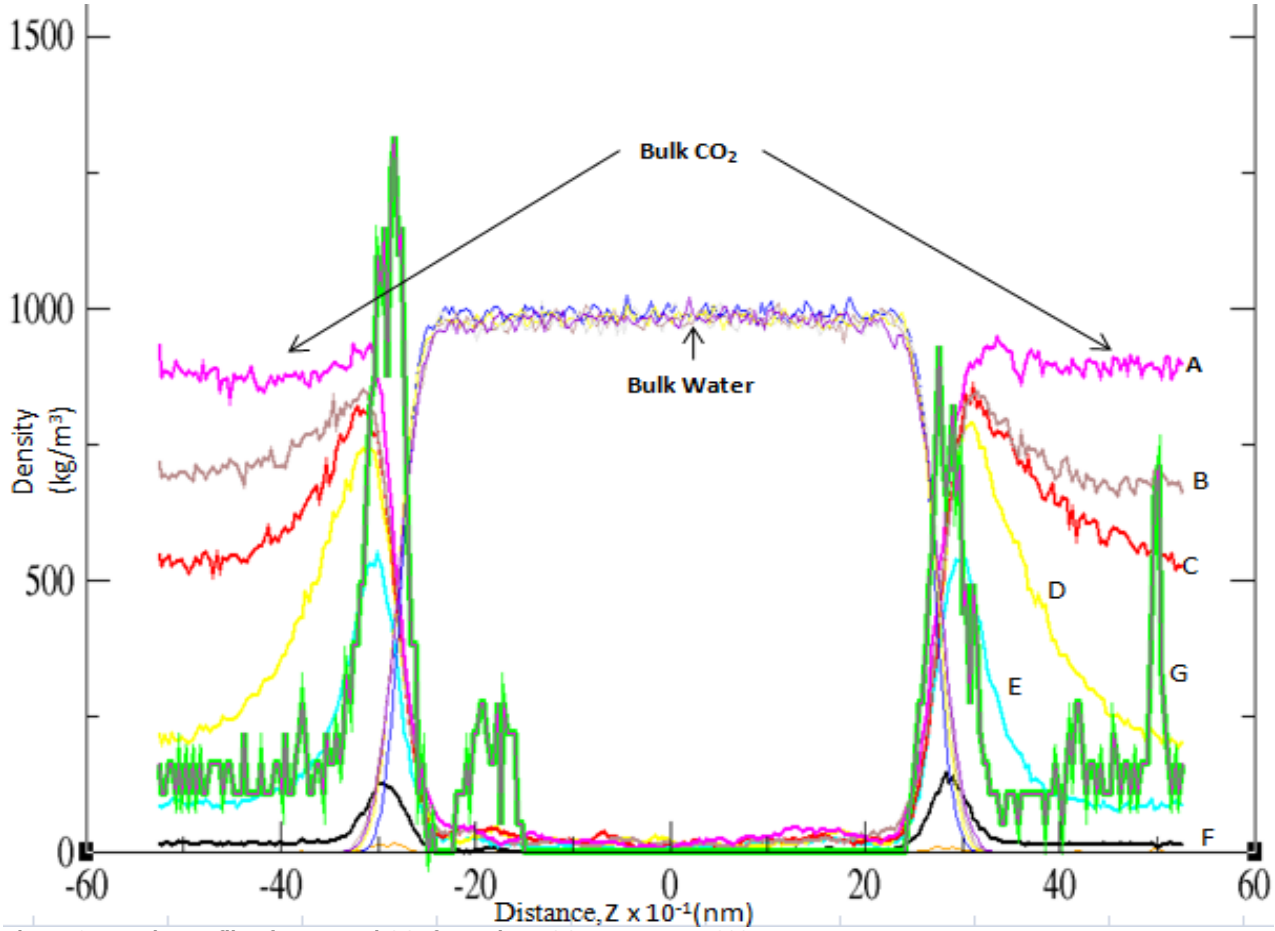

Figure 6: Density profile of water and CO_2 for various CO_2 pressure at 300 K.

CO_2 solubilities calculated from the MD simulation are compared with semi-empirical (Duan and Sun 2003) and experimental (Espinoza 2010) solubility data, Table 2 below. The force-field employed in this work under predicts the CO_2 solubilites.

Table 2: Comparison of solubilities obtained from MD simulation with solubilities calculated from Duan's(2003) model and Espinoza's (2010) experiment at 300K.

			Espinoza (298k)	
Pressure (MPa)	Solubility from simulation (mol/kg)	Solubility from Duan's calculation	Pressure (MPa)	Solubility (mol/kg)
0.85	0.11	0.26	0.10	0.03
3.94	0.28	0.98	6.40	1.38
6.13	0.43	1.29	10.00	1.42
5.81	0.5	1.26	20.00	1.56
7.36	0.42	1.36		
20.22	0.55	1.53		

Inorder to investigate the effect of temperature on the interfacial tensions computed with the MD model, two sets of simulations were run at 343.3K and 374.3K. All the other parameters used in these simulations are the same as previous simulations using the CO_2-water model at 300K.The results obtained are shown in the Figure 7 below; the model over predicts the interfacial tensions when compared to the experimental data of Georgiadis et al. (2010), but the over estimation is restricted to the water-liquid CO_2 interface. Result for the water-vapour phase CO_2 are quantitatively consistent with the experimental data.

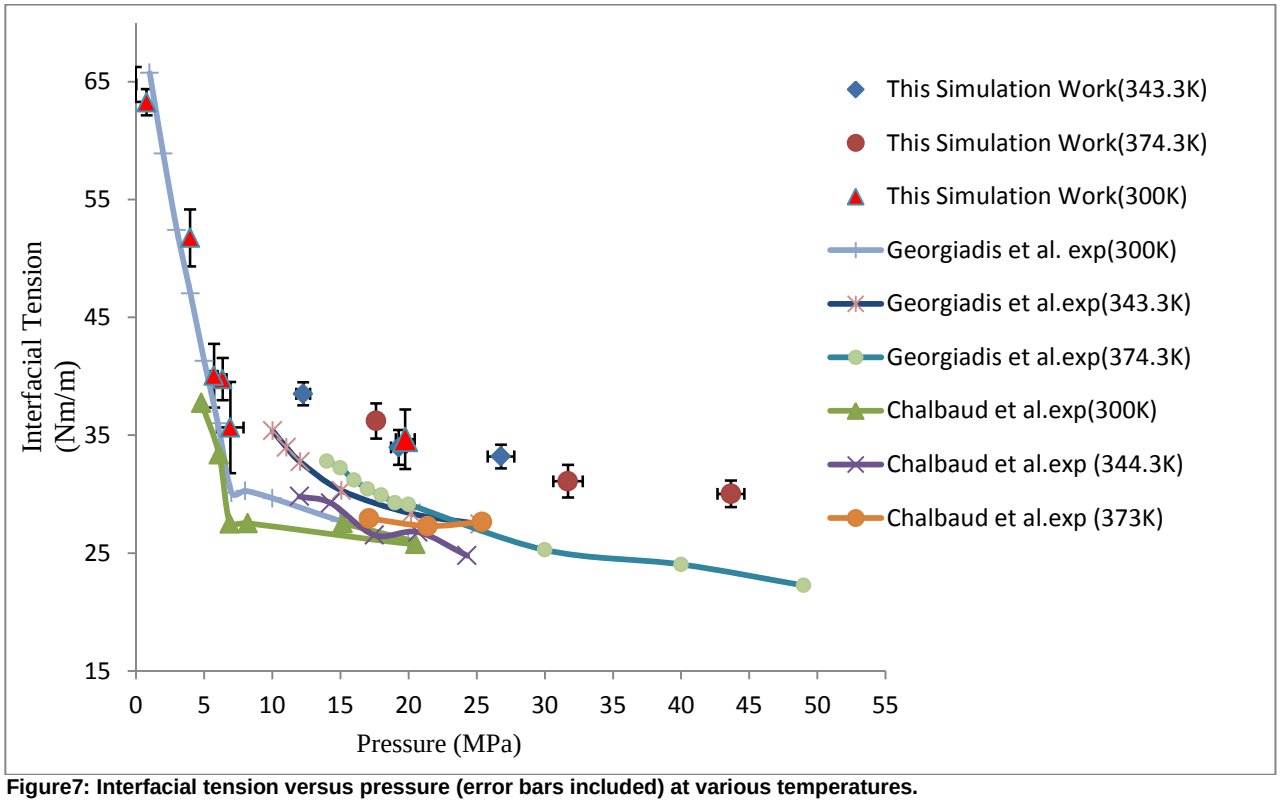

Figure7: Interfacial tension versus pressure (error bars included) at various temperatures.

Simulation Using the CO_2-Brine Model and Results: A CO_2-Brine model was developed by substituting water molecules by NaCl ion pairs in the configuration used in the CO_2-water model. The aim of introducing NaCl in the water was to investigate the influence of salinity on CO_2-water interfacial tension. The simulations were run for molarities ranging from 0.2M-3.5M which are relevant for CCS with all other parameters exactly the same as before. Simulations were run for 50000 steps to equilibriate the system.

From the Figures 8 and 9, it was found that the presence of salt decreases the total pressure of the system (this is because the simulation is performed with a constant box volume) ie, the pressure applied by CO_2 molecules onto the water interface. This is demonstrated in Figure 12 which indicates that the density of CO_2 in the bulk decreases with the increase in salt concentration.

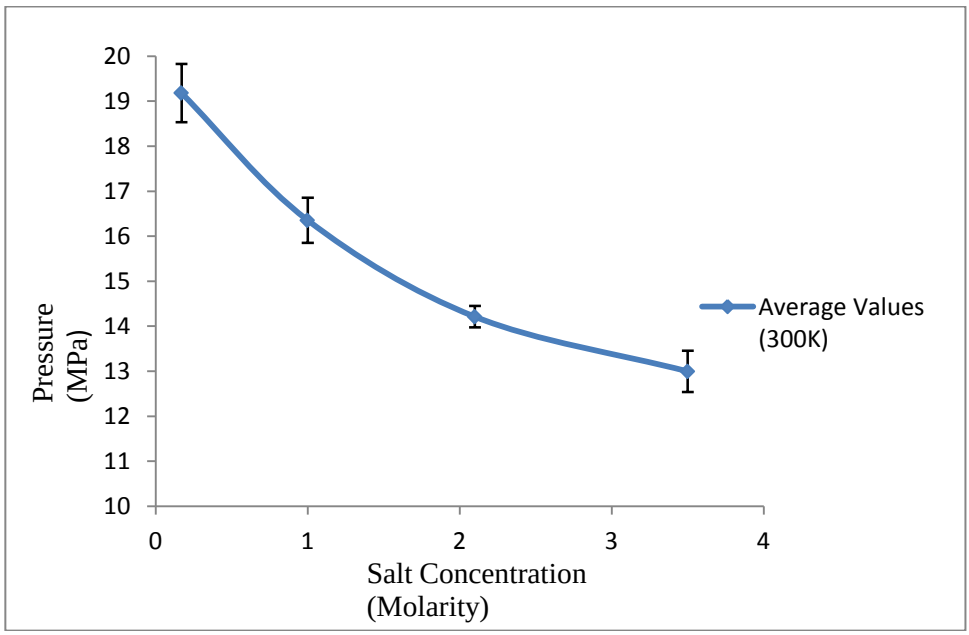

Figure 8: Pressure of CO_2 (system pressure-with error bars) vs NaCl concentration

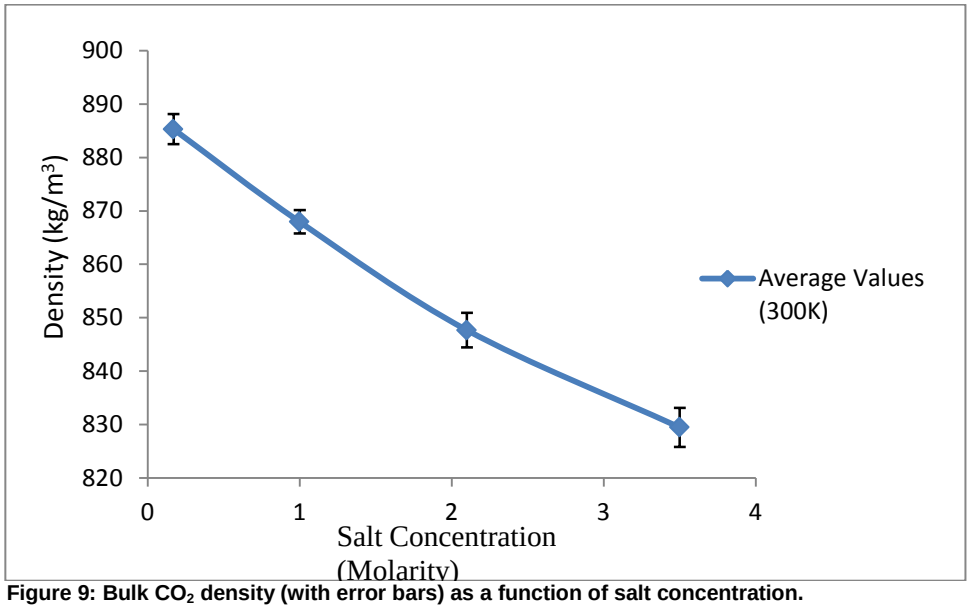

Figure 9: Bulk CO_2 density (with error bars) as a function of salt concentration.

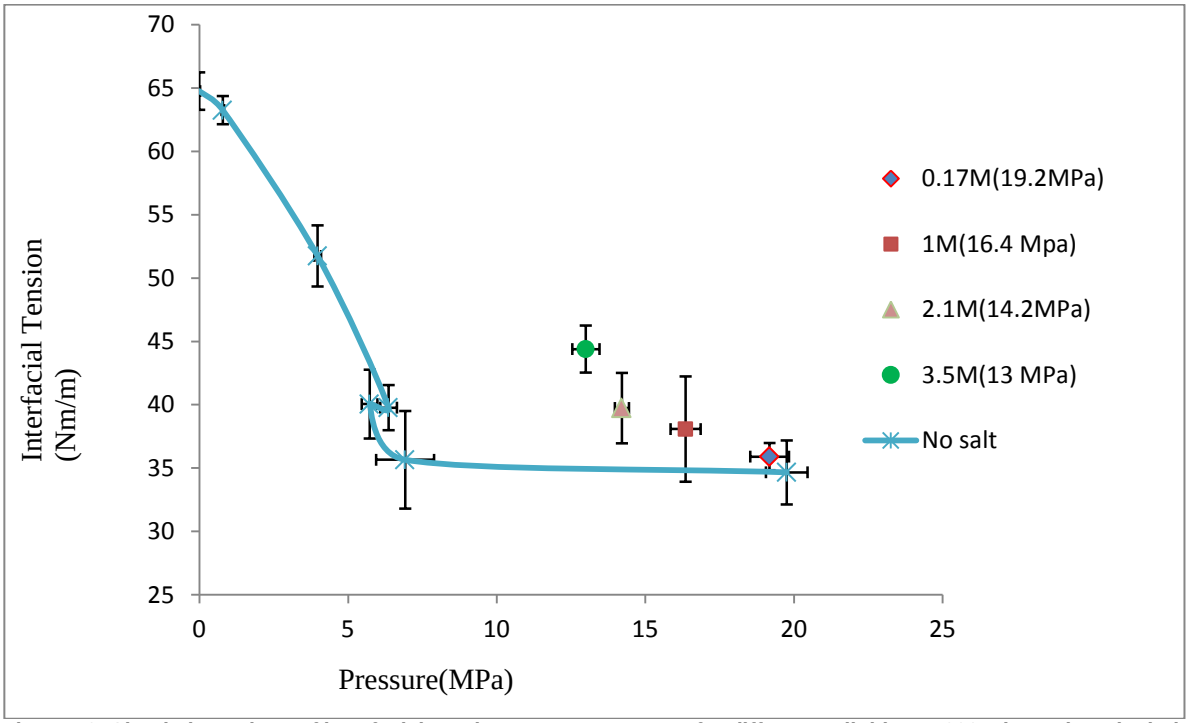

Figure 10: Simulation values of interfacial tensions versus pressure for different salinities at 300K (Error bars included).

Figure 10, shows an increase in computed interfacial tensions with addition of salt into the water, the maximum increase in this case for the highest salt concentration (3.5M).

Comparison of increase in interfacial tensions {IFT (salt) – IFT (no salt)} with Chalbaud et al. (2009) experiments (Figure 11) indicates that the increase in interfacial tensions (IFT) computed is an over prediction, the reason being that the CO_2-water model over predicts IFT values at same pressure and temperature conditions. However, the same trend of change in IFT is observed in both Chalbaud et al.'s experiment and in this simulation work. While Chalbaud et al.'s (2009) experiment shows an increase of 4mN/m in IFT for 2.8M salt concentration, simulation results shows an increase in IFT of 6mN/m.Hence, these results are comparable.

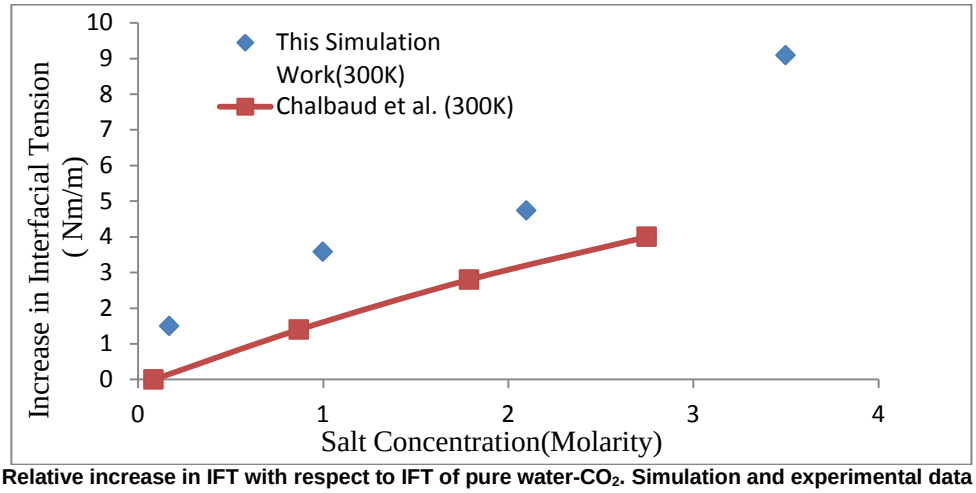

Figure 11: Relative increase in IFT with respect to IFT of pure water-CO_2. Simulation and experimental data are shown.

Figure 12 shows the density profiles of the simulations carried out on the brine-CO_2 system. The density profiles are calculated along the length of the simulation box. The dotted lines represent the densities of water, the dashed lines indicate CO_2 density and the continous lines the densities of NaCl solutions. It is clear from the Figure that the densities of CO_2 in the bulk decreases slightly with increase in salt concentration; this causes the increase in IFT. The bulk water density also decreases when salt is added.

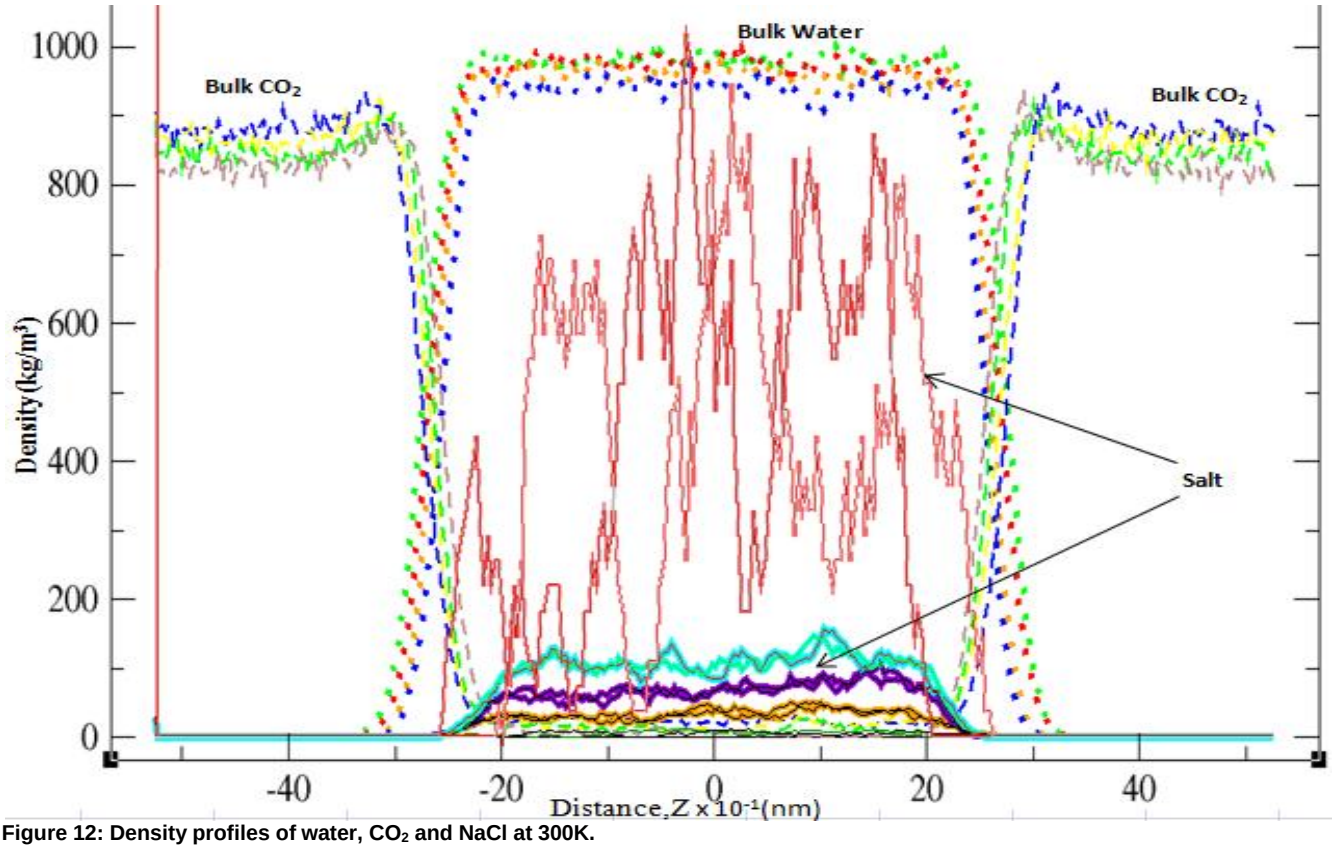

Figure 12: Density profiles of water, CO_2 and NaCl at 300K.

Bulk water (Dotted lines): Green- 0.17M, Red- 1M, Orange- 2.1M and Blue- 3.5M.
Bulk CO_2 (Dashed lines): Blue-19.93MPa and 0.17M, Yellow-16.51MPa and 1M, Green-13.82MPa and 2.1M and Brown-13.69MPa and 3.5M
NaCl ion pairs (Continous lines): Red-0.17M, Orange-1M, Violet-2.1M, Cyan (light blue)-3.5M,

Note that in Figure 12, the density values corresponding to the salt concentration of 0.17M is multiplied by a factor of 75 for better visualization.

Table 3: Values of CO_2 solubilities in brine computed with MD and with Duan's model (2003).

Molarity	Pressure (MPa)	Solubility from simulation (mol/kg)	Solubility from Duan's calculation (mol/kg)
0.17	19.9	0.53	1.47
1	16.5	0.38	1.2
2.1	13.8	0.28	0.93
3.5	13.7	0.14	0.72

Table 3 indicates that MD under predicts solubilities of CO_2 in brine computed through the simulation. This underprediction is a reflection of the solubility values underpredicted in the CO_2-water model. But the trend of decrease in solubility by the addition of salt is reproduced in the CO_2-brine model.

Simulation of the SiO_2-water System: As the first part of the second phase, an initial simulation was run on the SiO_2-water system (without CO_2, P_{CO2}=0) to check the water affinity of the silica surface used in the simulation. The cell used for the simulation contained a silica surface on which a water droplet is set up. The simulation used a box of dimension 7.902nm x 10.265nm x 15.0nm and was run in NVT ensemble at 300K. We employed 50000 steps with a timestep of 0.002ps to equilibrate the system. The vdW cutoff was set to 1.7nm. A total of 288 silicon, 288 oxygen atoms and 1000 water molecules were used for the simulation. Finally, the contact angle was measured by drawing iso-density lines which fitted the curvature of the droplet to form a circle (Figure 13). Then, the value of contact angle was calculated using equation 6. It was found that the silica surface used was hydrophilic in nature since a contact angle of 62.4^o was calculated. The simulated density profiles of quartz and water are shown in Figure 14.

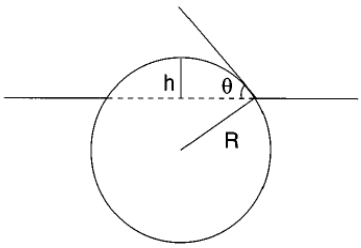

Figure 13: Contact angle calculation method (Bresme and Quirke 2000)

$$\cos\theta = 1-(h/R) \quad (6)$$

where,

h = height of the circle above the silica surface,

R= radius of the circle.

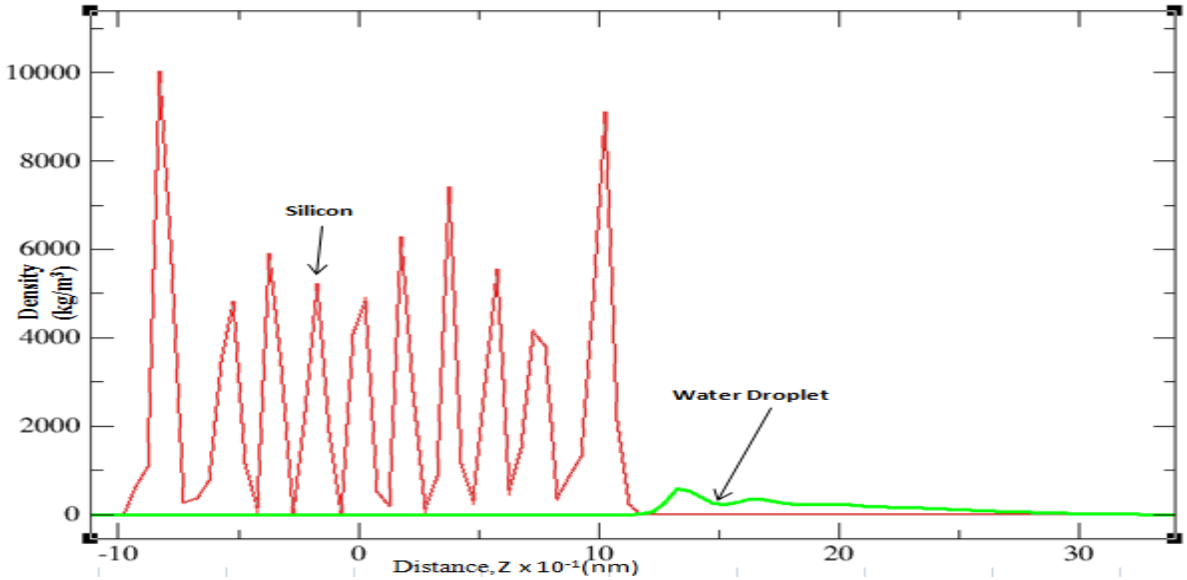

Figure 14: Density profiles of Quartz-Water simulation; silicon is red, water green at 300K.

Simulation of the SiO_2-water-CO_2 System: Two sets of simulations were run for this system. The first set investigated the influence of the pressure on contact angle and the second set investigated the effect of temperature on contact angle. A CO_2 repulsive barrier was introduced in the system to restrict the movement of CO_2 molecules into the other side of the box due to periodic boundary conditions. All parameters used for the simulation are exactly the same as used for the SiO_2-water system.

Figure 15 displays the values of contact angle obtained for various bulk CO_2 densities. The density of bulk CO_2 was obtained from Figure 16 below. These values show a similar trend to the one shown by Liu et al. (2010) at 318.15K, the reason being that in both the simulations a similar Si-O-Si bridged surface was used.

Figure 16 shows the density profile of CO_2, water and quartz. Water is represented by circles while CO_2 and silica (red) are represented by continous lines. The increase in CO_2 density from 27kg/m^3 to 895kg/m^3 resulted in an increase in the density profile of the water droplet on the quartz (light green circles to dark green circles). Further, this increase in radial density of the water droplet resulted in an increase in contact angle and is confirmed by the values of contact angles computed with isodensity lines (Bresme and Quirke 2000).

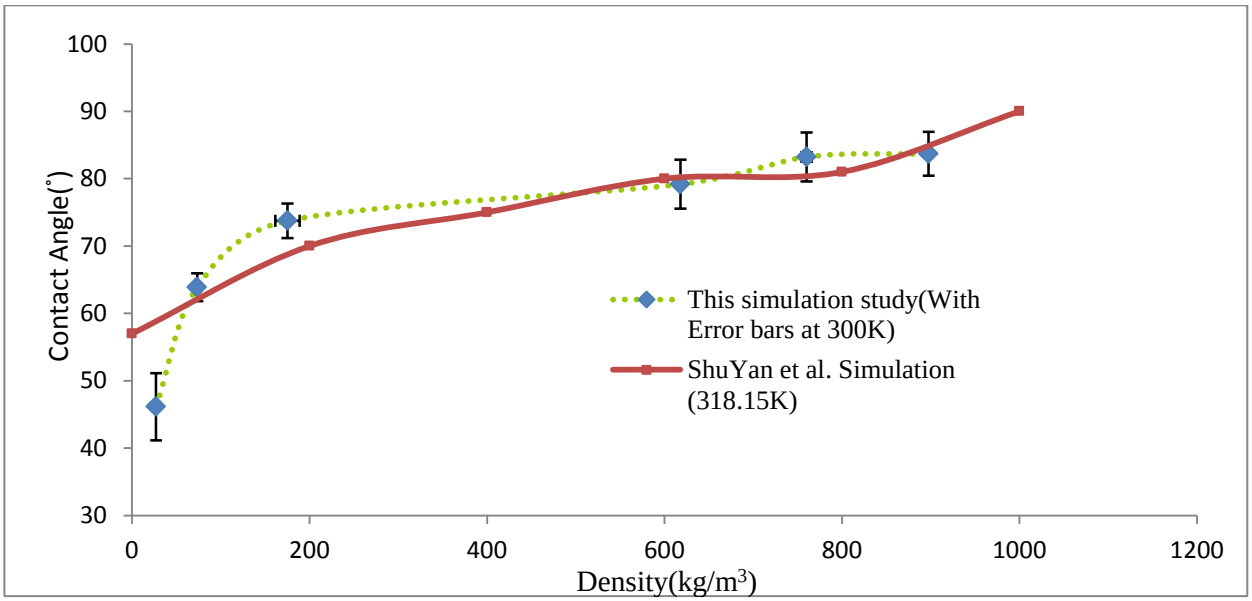

Figure 15: Contact angle versus CO_2 bulk density –weakly water wet (with error bars).

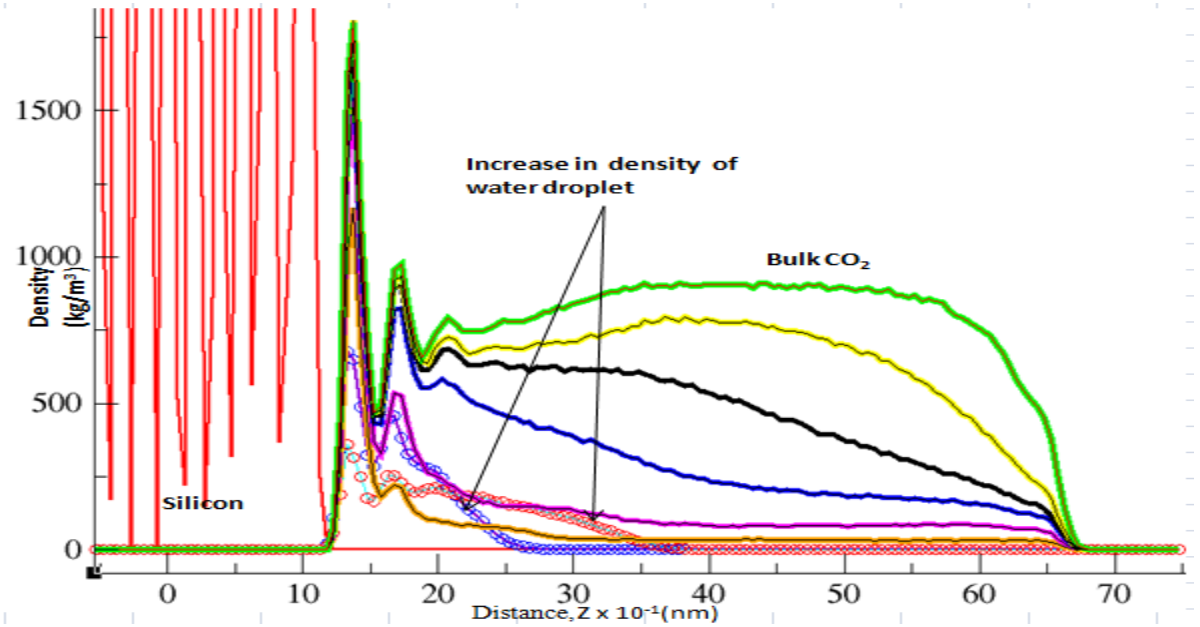

Figure 16: Density profile of CO_2, water and Silicon at 300K.

Where,

Bulk CO_2 (Continous line): Green-895kg/m^3, Yellow-762kg/m^3, Black-622kg/m^3,Blue-174kg/m^3, Magenta -78kg/m^3, Orange - 27kg/m^3 and Red – silicon.

Water Droplet (circles): Blue-27kg/m^3 and Red-895kg/m^3 (These curves are indicated by the arrows on the Figure 14)

In order to study the effect of typical reservoir temperatures on contact angle, two additional simulations were run at 320K and 350K in the NVT ensemble. The results are shown in Figure 17. It was found that with increasing temperature the density of bulk CO_2 decreased slightly which resulted in minute decrease in pressure from 19.5MPa to 19.0MPa (almost constant pressure) exerted by the bulk CO_2. But the contact angle remained almost constant. From this analysis, it is concluded that the temperature conditions typically found in the reservoir do not influence the contact angle significantly. Note that this simulation was run without any salt in the water droplet.

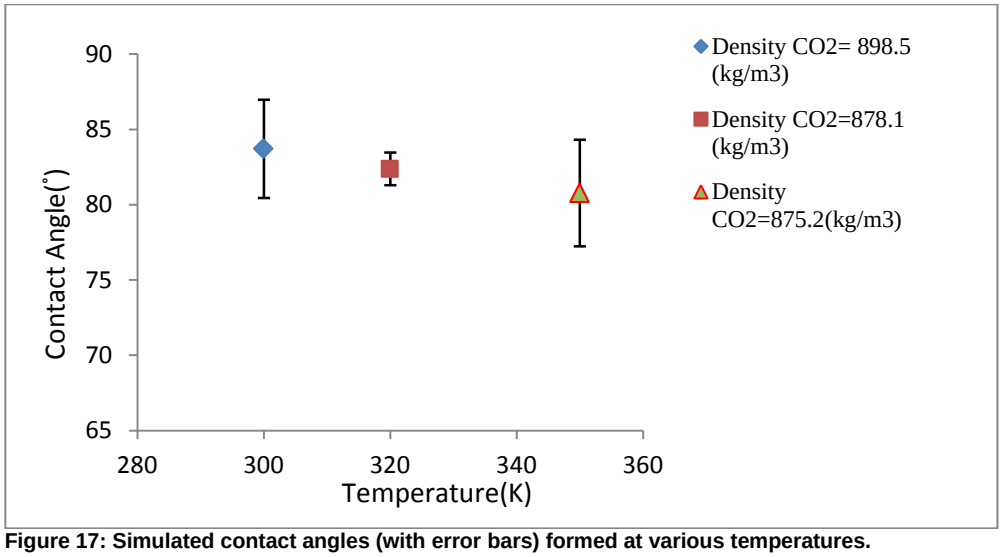

Figure 17: Simulated contact angles (with error bars) formed at various temperatures.

Simulation of the SiO_2-brine-CO_2 System: To investigate the influence of salt on contact angle, a set of four simulations were run for various molarities. All the simulation parameters were the same as for the SiO_2-water-CO_2 system except that new interaction parameters were introduced between quartz atoms and NaCl ions (Table C1). A total of 1200 molecules of CO_2 were used in each simulation. These parameters are listed in Table D 30 in the Appendix.

Figure 18 indicates that the computed contact angles increase drastically till the vapour-liquid boundary is reached. Once the CO_2 is liquid, the increase in contact angle with pressure becomes less rapid. The computed contact angles are a slight over prediction as the model underpredicts the CO_2 solubility in brine. The computed contact angles showed large variation (between 45^o-85^o) with the experimental results of Espinoza and Santamaria- around 20^o (2010) and Chiquet et al. – around 15^o-35^o (2007). This is because of the difference in substrate used in their experiments and in the presented simulations. If quartz is exposed to brine the silanol groups dissociate {point of zero charge is at pH = 3, (Bourikas et al. 2003)}; in addition an electrical double layer is formed at such a charged surface (Butt et al. 2006). The electrical double layer due to the quartz solution interface is considered in the simulation but the dissociation is not considered. Chiquet et al. (2007) established that there is not much effect of salt on contact angles in the case of quartz which is in agreement with the presented simulation work. However, Espinoza and Santamaria (2010)'s experimental values indicate an increase in contact angle of the order of 20 after the addition of small amounts of salt (0.2M). The MD results show that the contact angle increases with pressure, this trend is consistent with Chiquet et al. (2007) experimental data; but it is inconsistent with Espinoza and Santamaria (2010)'s data, which shows that the contact angle is constant versus pressure. However, it cannot be concluded that the experimental works of Espinoza and Santamarina are invalid since different substrates can show different behavior to various thermodynamic conditions.

In order to investigate the influence of brine-quartz surface interaction on contact angle, a simulation was run for 3.5M NaCl concentration by increasing the interaction parameters between the quartz atoms and NaCl atoms by a factor of 5. The result shows that the contact angle reduced from 69^o (lower interaction) to 49.4^o (higher interaction). Further, on comparing the density profile of these two simulations (Figure19), it was clear that the increased interaction of salt with quartz surface removed part of the CO_2 film adjacent to the quartz surface. This is indicated by the reduction in peak density of CO_2 (dashed brown lines to dashed magenta lines) and also by increase in peak density of NaCl ion pairs adjacent to the quartz surface. This reduction in CO_2 film at the silica surface contributed to the decrease in water droplet density and hence contact angle (from black circles to green circles).

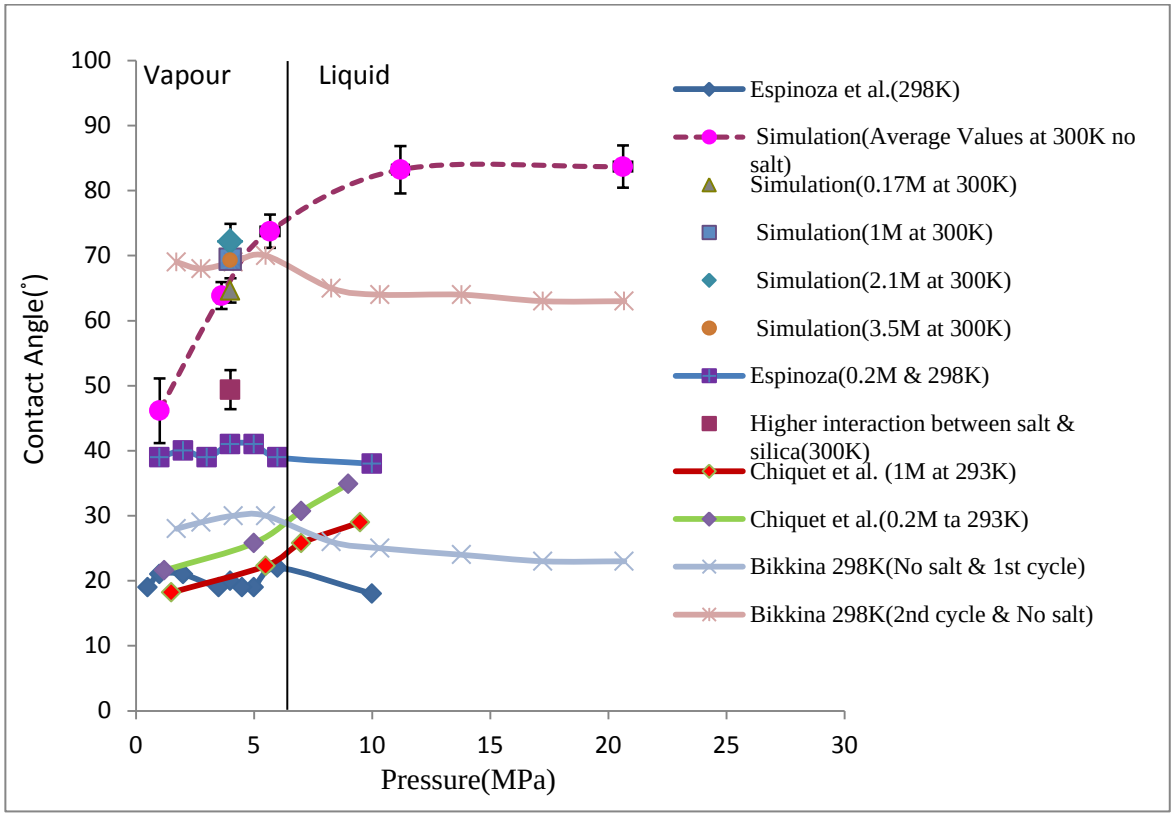

Figure 18: Simulated contact angles (with error bars) versus pressure for different salinities compared with experimental results at 300K.

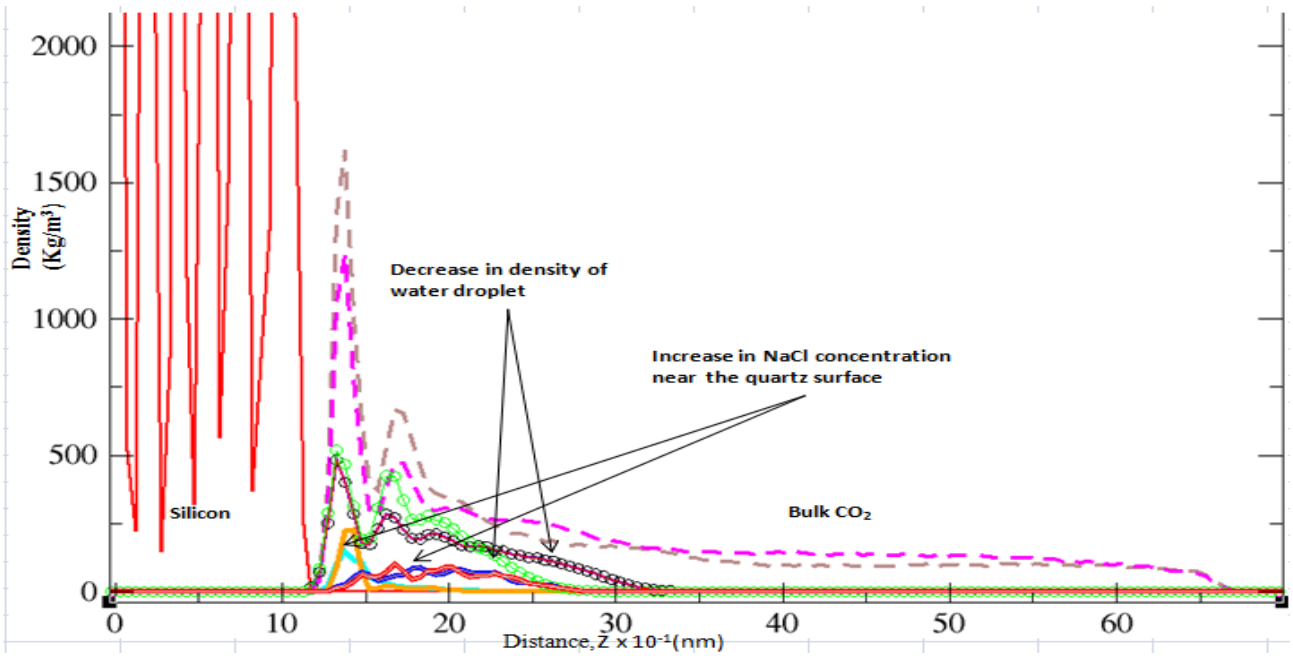

Figure 19: Density profiles of quartz, CO_2, water and salt at 300K

Where,

Bulk CO_2 (Dashed lines): Magenta-higher interaction between quartz and salt and Brown-lower interaction between quartz and salt.

Water Droplet (circles): Green-higher interaction between quartz and salt & Black-lower interaction between quartz and salt.

Salt (Continous lines): Red and Blue-salt with lower interaction with quartz (higher peak) and Orange and Cyan-salt with higher interaction with quartz (lower peak).

Note: Red and blue curves of salt are multiplied by a factor of 2 for better visualization.

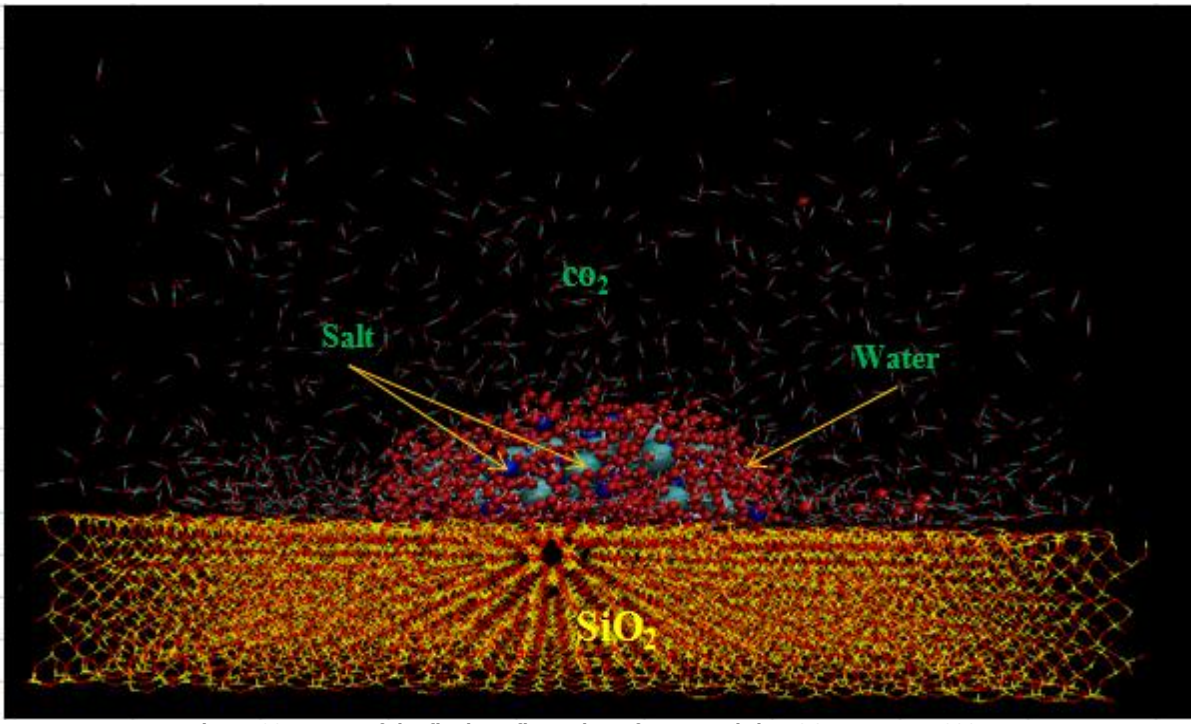

Figure 20: Image of the final configuration of a quartz-brine-CO_2 system at 300K.
(Yellow and red lines - SiO_2, Red spheres -Water, Light and dark blue spheres - NaCl, Red spheres with Blue lines - CO_2)

Discussion

The initial simulation study on the CO_2-water model established that the interfacial tension between CO_2 and water decreases with an increase in pressure till a pressure of 74bars is reached. This behaviour correlates well with the experimental values of CO_2-water interfacial tension. Our model represents better the interfacial tension of the CO_2-water interface than the simulation model of Zhang et al.(2011), and it is in better agreement with the experimental results of Chun- Wiliknson(1995) , Hebach et al.(2002), Georgiadis et al. (2010) and Chalbaud et al. (2009). However, the simulation over predicts the values of interfacial tension at high pressures, the calculated trend is nevertheless consistent with experimental results. It is clear from the presented results that for typical reservoir pressures and temperature conditions, the interfacial tension of the CO_2-water interface does not change significantly with pressure or temperature. However, the presence of salt increases the interfacial tension between water-CO_2 slightly, but the variation is small.This result is verified by the experimental results (Chalbaud et al. 2009). Since the contact angle is a function of interfacial tensions between CO_2-water, quartz-water and quartz-CO_2 (see equation 7), it has been shown that interfacial tension between CO_2 and water does not play a major role in the determinination of the contact angle.

$$\text{Cos } \theta = \frac{(\gamma_{CO2/SiO2} - \gamma_{Brine/SiO2})}{\gamma_{CO2/Brine}} \quad (7)$$

Where,

γ= interfacial tension.

The SiO_2-water (P_{CO2}=0MPa) simulation study found that a contact angle of 62.4^o is formed by the water droplet on the Si-O-Si bridged quartz surface. Hence the quartz surface investigated here is hydrophilic. The addition of CO_2 resulted in a signicant increase in this contact angle. It should be noted that quartz surfaces in a reservoir are more complicated because of dissociation of silanol groups and possible chemical heterogeneity. The simulation results by Liu et al. (2010) shows a similar trend in contact angles for a quartz-water-CO_2 system at 318.15K. The increased interaction of the salt with the quartz surface resulted in significant decrease in contact angle; i.e., contact angles are influenced significantly by the interaction between salt and quartz surface. Based on our results, we conclude that the contact angle is significantly influenced by the surface interaction between quartz-salt and quartz-CO_2. This cannot be inferred from experimental data as there are no accepted experimental methodologies with which solid-fluid interfacial tension can be measured directly.

Conclusions and Recommendations

A molecular dynamics simulation model has been developed which can compute contact angles of α-quartz (SiO_2)-water-CO_2 systems at any required pressures, temperature and salinity conditions.The effect of various interfacial tensions on contact angle were analysed and discussed. From this study we conclude:

- Molecular dynamics computer simulations are effective in computing contact angles for various thermodynamic

conditions and can be used as a tool to predict the approximate rock wettabilites.

- The CO_2-quartz interfacial interactions strongly influence the contact angle; more experimental and simulation works should be performed to investigate the CO_2-quartz system to obtain interfacial tensions and adsorption states of CO_2 films on the quartz surface at various thermodynamic conditions relevant to geological storage conditions.
- The molecular dynamics simulations can be extended to other mineral-CO_2-water interfaces such as calcite or mica.
- The predictions of CO_2-rock-brine contact angles help in assessing the effectiveness of the residual trapping mechanism.
- Through molecular dynamics simulation, we can compute the minimum pressure (threshold pressure or break through pressure) in the CO_2 phase which can initiate the displacement of brine from caprock.This can provide us with an estimate of CO_2 volume that can be stored in a reservoir by structural trapping.

Nomenclature

CCS	Carbon Capture and Storage
CO_2	Carbondioxide
SiO_2	Silicon dioxide, Quartz
H_2O	Water
PTFE	Poly tetra Fluoro Ethylene
vdW	Van der Waals
SiOH	Silicon Hydroxide, silanol
.17m	0 .17 Molality
M	Molarity
K	Degree Kelvin
Θ	Contact Angle
ɤ	Interfacial Tension
Kg	Kilogram
m^3	Cubic Metre
nm	Nano Meter
ε	Depth of Potential Well
σ	Distance at which the interparticle potential is zero
KJ	Kilo Joule
Mol	Moles
NaCl	Sodium Chloride
P_{XX}	Pressure in X direction
P_{YY}	Pressure in Y direction
P_{ZZ}	Pressure in Z direction
L_{ZZ}	Lateral Box Length
NVT	Canonical Ensemble
NPT	Isothermal Isobaric Ensemble
MPa	Mega Pascal
ASDA	Axisymmetric Drop Shape Analysis
OW	Oxygen Atom of Water Molecule
OC2	Oxygen Atom of Carbondioxide Molecule
HW	Hydrogen Atom of Water Molecule
OM	Imaginary Oxygen Atom In Water Molecule
C	Carbon Atom of Carbondioxide Molecule
Na	Sodium
Cl	Chlorine
Si	Silicon
O	Oxygen Atom of Silicon Dioxide Molecule
IFT	Interfacial Tension
Z	Radial Distance
P_{CO2}	Pressure of CO_2
MD	Molecular Dynamics
A	Alpha
exp	Experiment

Acknowledgement

I would like to thank my supervisors Fernando Bresme and Stefan Iglauer for their immense help and support technically and mentally. This project would not have been possible without their exceptional mentoring and valuable inputs of knowledge. I would also like to extend my heartfelt appreciation to Dr.Frank Romer, Serapian Stefano, Wendy Zhang, Sebastian Kutsch and Jordan Muscatello for spending their precious time answering my questions and helping me solve the problems encountered during the course of the project. I would also like to offer my gratitude to the Imperial College authorities for giving me the opportunity to do this project.

References

Abascal, J. L. F. and Vega, C.:"A General Purpose Model For Condensed Phases of Water: TIP4P/2005", *The Journal of Chemical Physics*, **123**, 234505, 2005.

Adeagbo, W.A., Doltsinis, N. L., Klevakina, K. and Renner, J.: "Transport Processes at α-Quartz-Water Interfaces- Insights from First Principles Molecular Dynamics Simulation", *ChemPhysChem*, **9,** 994-1002, 2008.

Alder, B. J., and Wainwright, T. E.:"Studies in molecular dynamics. I.General method", J. Chem. Phys, **31**,459–466, 1959.

Allen, M.P. and Tidesley, D. J.:"*Computer Simulation of Liquids"*, Oxford Science Publications, Oxford, 1989.

Atkins, P. and de Paula, J.: "*Atkins' Physical Chemistry*", 7th Edition, Oxford University Press, 2002.

Bharatwaj, B. and Rocha, S. R. P:" Interfacial Phenomenon At The compressed CO_2-Water Interface", *Brazilian Journal of Chemical Engineering*, **23**(02), 183-190, 2006.

Bikkina, P. K.: "Contact angle measurements of CO_2-H_2O-quartz/calcite systems in perspective of carbon sequestration", *International Journal of Greenhouse Gas Control* -414, 2011.

Bourikas, K., Vakros, J., Kordulis, C., Lycourghiotis, A.: "Potentiometric mass titrations: experimental and theoretical Establishment of a new technique for determining the point of zero charge of metal hydroxides ", *Journal of Physical Chemistry B*, **107**, 9441-9451, b 2003.

Bresme, F. and Quirke, N.: "Computer Simulation Studies of Liquid – Liquid Denses at a Liquid – Liquid Interface", *Journal of Chemical Physics*, **112**(13), 5985-5990, 2000.

Butt, H.J., Graf, K. And Kappl, M.,:"*Physics and Chemistry of Interfaces*", Darmstadt: Wiley-VCH, 2006.

Chalbaud, C. , Robin, M., Lombard, J. M., Martin, F., Egermann, P. and Bertin, H.: "Interfacial tension measurements and wettability evaluation for geological CO_2 storage", *Advances in Water Resources*, **32**, 98-109, 2009.

Chiquet, P., Broseta, D. and Thibeau, S.: "Wettability alteration of caprock minerals by CO_2 ", *Geofluids*, **7**, 112-122,(2007).

Chun, B.-S.; Wilkinson:"Interfacial Tension In High Pressure Carbondioxide Systems", *G. T. Ind. Eng. Chem. Res.*, **34**(12), 4371–4377, 1995.

Cole, D. R., Chialvo, A. A., Rother, G., Vlcek, L. and Cummings, P.T. : "Supercritical Fluid Behaviour at Nanoscale Interfaces - Implications for CO_2 Sequestration in Geologic Formations", *Philosophical Magazine*, **90**(17), 2339-2363, 2010.

da Rocha, S. R. P., Johnston, K. P. and Rossky, P. J.:" Surfactant-Modified CO_2-Water Interface: A Molecular View", *J. Phys. Chem B*, **106**, 13250-13261, 2002.

Dickson, J. L., Gupta, G., Horozov, T. S., Binks, B. P. and Johnston, K. P.: "Wetting phenomenon at the CO_2/water/glass interface", *Langmuir*, **22**, 2161-2170. 2006.

Duan Z.H and Sun R.:"An improved model calculating CO_2 solubility in pure water and aqueous NaCl solutions from 273 to 533 K and from 0 to 2000bar", *Chem. Geology***,** vol. **193**, pp 253-271, 2003.

Espinoza, D.N. and Santamarina, J.C.: "Water-CO_2-mineral systems: Interfacial tension, contact angle and diffusion- Implications to CO_2 geological storage", *Water Resources Research*, **46**, W0753, 2010.

Georgiadis, A., Maitland, G., Trusler, J. P. M. and Bismarck, A.:" Interfacial Tension Measurements of the (H_2O + CO_2) System at Elevated Pressures and Temperatures", *J. Chem. Eng. Data*, *55***,** 4168-4175,2010.

Harris, J.G. and Yung, K.H.:"Carbon Dioxide's Liquid-Vapour Coexistence Curve and Critical Properties As Predicted by a Simple Molecular Model", *J.Phys.Chem.*, **99**(31), 12021-12024, 1995.

Hebach, A., Oberhof, A., Dahmen, N., Kogel, A., Ederer, H. and Dinjus:"Interfacial Tension at Elevated Pressures: Measurements and Correlations in the Water + Carbon Dioxide System", *J. Chem. Eng. Data*, **47** (6), 1540–1546, 2002.

Kraska, T., Romer, F. and Imre, A. R.:"The Relation of Interface Properties and Bulk Phase Stability- Molecular Dynamics Simulations of Carbondioxide", J. *Phys. Chem. B*, **113**, 4688-4697, 2009.

Kvamme, B., Kuznetsova, T., Hebach, A., Oberhof, A. and Lunde, E.: "Measurements and Modelling of Interfacial Tensions For Water + Carbondioxide Systems at Elevated Pressures", *Computational Materials Science*, **38** 506-513, 2007.

Lopes, P. E. M., Murashov, V., Tazi, M., Demchuk, E. and Mackerell, A. D.: "Develeopmentof an Emperical Force Field for Silica. Application to the Quartz- water Interface", *J. Phys. Chem. B*, **110**, 2782-2792, 2006.

Naylor, M., Wilkinson M. and Hazeldine, R.S.:"Calculation of CO_2 column heights in depleted gas fields from known pre-production gas column heights", *Marine and Petroleum Geology*, **28**, 1083-1093, 2011.

Pentland, C. H., El-Maghraby, R., Iglauer, S. and Blunt, M. J. :" Mesaurements of the Capillary Trapping Of Super - Critical Carbondioxide in Berea Sandstone", *Geophysical Research Letters*, **38**, L06401, 2011.

Plug, W. J. and Bruining, J.: "Capillary Pressure for the Sand- CO_2-Water System under Various Pressure Conditions. Application to CO_2 Sequestration", *Advances In Water Resources*, **30**, 2339-2353, 2007.

ShuYan, L., XiaoNing, Y. and Yan, Q.:"Molecular dynamics simulation of wetting behaviour at CO_2/water/solid interfaces", *Chinese science Bulletin*, Vol.55**,** No.21, 2252-2257, 2010.

Smith, W., Forester, T.R. and Todorov, I. T.:"*The Dl_POLY/2.19 User Manual*", STFC DaresburyLaboratory, Cheshire, UK, 2008.

Span, R and Wanger, W.: "Equations of State for Technical Applications. I. Simultaneously Optimized Functional Forms for Nonpolar and Polar Fluids", *Int. J. Thermophys.*, ***24(1)***, 1-39, 2003.

Spiteri, E.J., Juanes, R., Blunt, M. J., Franklin M.Orr, Jr.: "A New Model of Trapping and Relative Permeability Hysterisis for All Wettability Characteristics ", *SPE Journal*, **13**(3), 277-288, 2008.

van Beest, B.W.H., Kramer, G.J. and van Santen R.A.: "Force Fields for Silicas and Aluminophosphates Based on Ab Initio Calculations ", *Physical Review Letters*, **64**(1990).

Yang, D.,YonganGu and Tontiwachwuthikul, P.:" Wettability determination of the reservoir brine-reservoir rock-system with dissolution of CO_2 at high pressures and elevated temperatures", *Energy and Fuels*, **22**, 504-509, 2008.

Zhang, H. and Singer, S. J. :"Analysis of Subcritical Carbon Dioxide – Water Interface", *J. Phys. Chem A*, **115**, 6285-6296, 2011.

APPENDICES

APPENDIX A Critical Literature Review

Table A 1: Important milestones in the study of contact angles between mineral/water/CO_2.

Date	Title	Authors	Contributions
31st March 2011	Contact angle measurements of CO_2-H_2O-quartz/calcite systems in perspective of carbon sequestration	Prem Kumar Bikkina	Presented contact angle measurements for CO_2-H_2O-quartz/calcite systems and investigated the influence of drop volume, pressure, temperature and repeated exposure of dense water saturated CO_2 on contact angle.
25th March 2011	Analysis of the Sub Critical Carbon Dioxide-water Interface	Hui Zhang and Sherwin. J. Singer	First to do molecular dynamics simulation to obtain CO_2-water interfacial tension using SPCE water model and EPM2 carbondioxide model.
29thJuly 2010	Water-CO_2-mineral systems: Interfacial tension, contact angle and diffusion-Implications to CO_2 geological storage	D.Nicolas Espinoza and J.CarlosSantamarina	Extended the scope of previous studies to include other substrates {quartz, calcite, oil wet quartz, polytetrafluoroethylene (PTFE)} and pore fluid conditions that may be encountered in natural systems in context of CO_2injectability and storage in geological formations.
15th April 2010	Molecular dynamics simulation of wetting behavior at CO_2/water/solid interfaces	LIU Shu Yan, YANG XiaoNing& QIN Yan	First to use molecular dynamics simulation to demonstrate the microscopic wetting behavior of hydrophobic and hydrophilic surfaces in a dense CO_2 fluid environment under various densities.
29th October 2008	Interfacial tension measurements and wettability evaluation for geological CO_2 storage.	Chalbaud et al.	Presented brine-CO2 interfacial tension datas for temperature, pressure and salt concentrations similar to that of a saline aquifer.
16th October 2007	Wettability determination of the reservoir brine-reservoir rock-system with dissolution of CO_2at high pressures and elevated temperatures.	Daoyong Yang, YonganGu and PaitoonTontiwachwuthikul	Developed an experimental method to determine the wettability of reservoir brine –reservoir rock system with dissolution of CO_2 at high pressures and elevated temperatures by using axisymmetric drop shape analysis technique.
19th December 2006	Wettability alteration of caprock minerals by CO_2	P.Chiquet, D.Broseta and S.Thibeau	Conducted contact angle measurements for brine/CO_2/mica &quartz systems.
16th December 2005	Wetting phenomenon at the CO_2/water/glass interface	Jasper L.Dickson, Gaurav Gupta, Tommy S.Horozov, Bernard P.Binks& Keith P.Johnston	Developed a novel high pressure apparatus and technique to measure CO_2/water/2 glass substrates contact angles in situ for pressures up to 204bar.

APPENDIX A-1 Paper Review

International Journal of Greenhouse Gas Control -414

Contact angle measurements of CO_2-water-quartz/calcite systems in the perspective of carbon sequestration.

Author: Prem Kumar Bikkina

Contribution to the understanding of molecular dynamics simulation model for SiO_2-water-CO_2sytem
Presented contact angle measurements for CO_2-H_2O-quartz/calcite systems and investigated the influence of drop volume, pressure, temperature and repeated exposure of dense water saturated CO_2 on contact angle.

Objective of the paper:
To investigate the influence of drop volume, repeated exposure of substrates to dense water saturated CO_2, pressure and temperature on the contact angles formed between CO_2-water-quartz/calcite system.

Conclusion reached:
He concluded that the there was no effect of drop size on contact angle but repeated exposure of dense water saturated CO_2 significantly altered the contact angle trends. Contact angle increased slightly with pressure and span (contact angle before and after experiment) of contact angle decreased with temperature.

Comments:
The effect of salt on contact angle is not considered which is very relevant to reservoir conditions.

J.Phys.Chem. A 2011, 115, 6285-6296

Analysis of the Sub Critical Carbon Dioxide- Water Interface

Author: Hui Zhang and Sherwin. J. Singer

Contribution to the understanding of molecular dynamics simulation model for SiO_2-water-CO_2 system
First to do molecular dynamics simulation to obtain CO_2-water interfacial tension using SPCE water model and EPM2 carbondioxide model.

Objective of the paper:
To present the evolution of interfacial properties of CO_2-water at 300K and validate it with experimental results.

Methodology used:
The DL_POLY 2 molecular dynamics simulation package was used to simulate the CO_2/water interface using the potential SPCE water model and EPM2 carbondioxide model.

Conclusion reached:
The CO_2 film density profile was seen to grow linearly with bulk CO_2 density, till a density of 0.00095x $10^{-3}nm^3$ is reached. A second peak of CO_2 was observed at pressures higher this point.

Comments:
The interfacial energy is under estimated by these models.

Water Resources Research, Vol.46, W07537

Water-CO_2-mineral systems: Interfacial tension, contact angle and diffusion-Implications to CO_2 geological storage.

Author: D.Nicolas Espinoza and J.CarlosSantamarina

Contribution to the understanding of molecular dynamics simulation model for SiO_2-water-CO_2sytem
Extended the scope of previous studies to include other substrates {quartz, calcite, oil wet quartz, polytetrafluoroethylene (PTFE)} and pore fluid conditions that may be encountered in natural systems in context of CO_2injectability and storage in geological formations.

Objective of the paper:
To understand the evolution of contact angle for various pressure, salinity conditions, substrates and to evaluate the underlying the mechanism of contact angle formation.

Methodology used:
The sessile drop method was used to understand the evolution of interfacial tension and contact angle.

Conclusion reached:

1. Interfacial tension decreased with increasing CO_2 pressure.
2. Contact angle was seen to increase wih oil wet surfaces but decreases in case of water wet surfaces.

Comments:
The results do not agree well with the work of Chiquet et al. (2006) and Daoyong Yang et al. (2007).

Chinese Science Bulletin, Vol.55, No.21:2252-2257

Molecular dynamics simulation of wetting behavior at CO_2/water/solid interfaces

Author: LIU Shu Yan, YANG XiaoNing& QIN Yan

Contribution to the understanding of molecular dynamics simulation model for SiO_2-water-CO_2sytem
First to use molecular dynamics simulation to demonstrate the microscopic wetting behavior of hydrophobic and hydrophilic surfaces in a dense CO_2 fluid environment under various densities.

Objective of the paper:
To demonstrate the wettability behavior of water on the quartz surface under CO_2 pressure using molecular dynamics and explain the underlying mechanism.

Methodology used:
Molecular dynamics simulation was performed using the SPCE water model and single point model for CO_2.

Conclusion reached:

1. The water droplet loses contact from a hydrophobic surface under high CO_2 density.
2. The contact angle was seen to increase with CO_2 density but no separation was observed.

Comments:
The model does not explain the influence of salinity and temperature on contact angle.

Advances in Water Resources 32(2009) 98-109

Interfacial tension measurements and wettability evaluation for geological CO_2 storage.

Author: C. Chalbaud, M. Robin, J. M. Lombard, F. Martin, P. Egermann, H.Bertin.

Contribution to the understanding of molecular dynamics simulation model for SiO_2-water-CO_2sytem
Presented brine-CO_2 interfacial tension datas for temperature, pressure and salt concentrations similar to that of a saline aquifer.

Objective of the paper:
To study the wettability at the pore scale using glass micromodels.

Methodology used:
Axi-symmetric drop shape analysis was used to acquire images of a drop and the drop profile using the edge detection techniques.

Conclusion reached:

1. In strongly hydrophilic surface, the CO_2 does not wet the surface.
2. In less hydrophilic porous surface, the CO_2 significantly wets the surface.

Comments:
Inappropriate to draw out conclusions based on this work in the case of reservoir caprocks.

Energy and Fuels 2008, 22, 504-509

Wettability determination of the reservoir brine-reservoir rock-system with dissolution of CO_2at high pressures and elevated temperatures.

Author: Daoyong Yang, YonganGu and PaitoonTontiwachwuthikul

Contribution to the understanding of molecular dynamics simulation model for SiO_2-water-CO_2sytem
Developed an experimental method to determine the wettability of reservoir brine –reservoir rock system with dissolution of CO_2 at high pressures and elevated temperatures by using axisymmetric drop shape analysis technique.

Objective of the paper:
To determine the wettability of a reservoir bribe=reservoir rock system with CO_2 dissolution at high pressures and temperatures.

Methodology used:
Axi-symmetric drop shape analysis for the sessile drop case is used to determine the dynamic and equilibrium contact angle.

Conclusion reached:

1. The dynamic contact angle between the reservoir brine and the reservoir rock almost remains constant at a given pressure and constant temperature.
2. The equilibrium contact angle increases with pressure and decreases with temperature.

Comments:
Contradicts the work of D.Nicolas Espinoza and J.CarlosSantamarina.

Geofluids (2007) 7, 112-122

Wettability alteration of caprock minerals by CO_2

Author: P.Chiquet, D.Broseta and S.Thibeau.

Contribution to the understanding of molecular dynamics simulation model for SiO_2-water-CO_2sytem
Conducted contact angle measurements for brine/CO_2/mica &quartz systems.

Objective of the paper:
To obtain the experimental evidence to prove that the wettability of mica and quartz substrates is altered by the presence of CO_2 under pressure conditions similar to geological storage.

Methodology used:
Captive drop technique was used to measure advancing contact angle and receding contact angle.

Conclusion reached:
Wettability of caprock is altered by increase in CO_2 pressure due to reduction in brine pH.

Comments:
Contradicts the work of D.Nicolas Espinoza and J.CarlosSantamarina.

Langmuir 2006, 22, 2161-2170

Wetting phenomenon at the CO_2/water/glass interface

Author: Jasper L.Dickson, Gaurav Gupta, Tommy S.Horozov, Bernard P.Binks& Keith P.Johnston

Contribution to the understanding of molecular dynamics simulation model for SiO_2-water-CO_2sytem
Developed a novel high pressure apparatus and technique to measure CO_2/water/2 glass substrates contact angles in for high pressures.

Objective of the paper:
To obtain the wettability charactersistics of 2 glass substrates of different hydrophilicities for various pressures exerted by CO_2 and also to investigate the influence of long and short range interactions with the silanol groups on contact angle and interfacial tension.

Methodology used:
A high pressure apparatus was used which consists of a high pressure view cell, an optical rail, a CCD camera and a port at the bottom for a removable stage.

Conclusion reached:
Contact angle hysteresis was discovered in which larger θ values where observed during depressurization than during pressurization.

Comments:
Substrates and thermodynamic conditions used in this work are not relevant to reservoir conditions.

APPENDIX B Background on TIP4P-2005 and EPM2 Models.

TIP4P-2005 Water Model

The TIP4P-2005 is a potential model for the condensed phases of water developed by J. L. F Abascal and C. Vega (2005). This is a rigid 4 site model with 3 fixed point charges and one Lennard-Jones center. Various thermodynamic properties of solid and liquid phases were calculated using this model.The properties calculated covered a temperature range from 123K to 573K and pressures upto 4000MPa. The model predicts the water densities at 1bar with a maximum density at 278K and an averaged difference with experiment of 0.7 kg/m^3.

EPM2 CO_2 Model

The EPM2 model is a rigid site based intermolecular potential model for CO_2 developed by Harris and Yung (1996).In this model the CO_2 molecule is represented by 3 Lennard Jones sites and 3 partial charges at the same positions.The EPM2 model predicts the coexistence curve and critical properties of CO_2 quite close to the experimental values.

APPENDIX C Lennard Jones Potential Parameters and Buckingham Potential Parameters (Allen et al. 1989)

Table C1: Lennard Jones potential parameters used in the simulations.

Atoms	ε(KJ/mol)	σ x 10^{-1}(nm)
Si - OW	.643019	3.4769
Si - HW	0	1
Si - OM	0	1
O - OW	.709053	3.15645
O - HW	0	1
O - OM	0	1
OW – OW	0.77502	3.1589
OW – HW	0.0	1.0
OW – OM	0.0	1.0
HW – HW	0.0	1.0
HW – OM	0.0	1.0
OM - OM	0	1
C - C	.23391	2.757
C - OC2	.39572	2.895
OC2 - OC2	.66947	3.033
OW – C	0.42576	2.95795
OW – OC2	0.72031	3.09595
HW – C	0.0	1.0
HW - OC2	0	1
OM - C	0	1
OM - OC2	0	1
Si - C	.35326	3.276
Si - OC2	.59763	3.414

O - C	.38953	2.9555
O - OC2	.659	3.0935
OW - NA	.38975	2.80445
OW - CL	.69765	3.62945
HW - NA	0	1
HW - CL	0	1
OM - NA	0	1
OM - CL	0	1
C - NA	.21412	2.6035
C - CL	.38327	3.4285
OC2 - NA	.36224	2.7415
OC2 - CL	.6484	3.5665
NA - NA	.196	2.45
CL - CL	.628	4.1
NA - CL	.35084	3.275
Si - NA	.3233	3.1225
Si - CL	.57883	3.9475
O - NA	.35657	2.802
O - CL	.638266	3.627

Table C2: Buckingham potential parameters (A, B, C are Buckingham constants).

Atoms	A(kJ/mol)	B x10 $(nm)^{-1}$	C {(kJ/mol) (nm^6)}
Si - Si	0	1	0.0
Si - O	1.7373 E+06	.2052	.012886
O - O	134011.75	.3623	0.016887

APPENDIX D Results of the CO_2-water, CO_2-brine, SiO_2-water-CO_2 and SiO_2-brine-CO_2 simulations.

Table D 1: Results of first run using CO_2-water model at 300K.

RUN1	Pressure Tensors						
No: of CO_2 molecules used	P_{XX} (MPa)	P_{yy} (MPa)	P_{ZZ} (MPa)	$P_{correction}$ (MPa)	Total System Pressure (MPa)	Interfacial Tension (mN/m)	Density (Kg/m^3)
10	-13.44	-14.16	-1.32	-1.31	-0.01	65.87	1.48
100	-12.74	-12.52	-0.61	-1.39	0.78	63.44	17.77
512	-7.27	-6.82	2.27	-1.80	4.06	49.13	99.18
1024	-2.79	-4.08	4.47	-2.38	6.85	41.74	254.25
1500	-4.82	-5.68	2.58	-2.99	5.57	41.30	553.80
1700	-1.79	-1.95	5.01	-3.27	8.28	36.28	662.59
2048	10.66	9.71	16.94	-3.78	20.72	35.67	888.16

Table D 2: Results of second simulation run using the CO_2-water model at 300K.

RUN2	Pressure Tensors						
No: of CO_2 molecules used	P_{XX} (MPa)	P_{yy} (MPa)	P_{ZZ} (MPa)	$P_{correction}$ (MPa)	Total System Pressure (MPa)	Interfacial Tension (mN/m)	Density (Kg/m^3)
10	-13.89	-13.67	-1.28	-1.31	0.03	65.96	1.77
100	-12.90	-12.08	-0.67	-1.39	0.72	62.40	16.42
512	-7.70	-7.22	2.15	-1.80	3.95	50.73	86.87
1024	-3.33	-3.79	3.85	-2.38	6.22	39.07	234.84
1500	-4.24	-4.62	3.17	-2.99	6.16	40.09	544.59
1700	-3.42	-3.32	3.09	-3.27	6.36	34.09	692.85
2048	9.88	9.63	15.80	-3.78	19.59	31.92	895.13

Table D 3: Results of third simulation run using the CO_2-water model at 300K.

RUN 3	Pressure Tensors						
No: of CO_2 molecules used	P_{XX} (MPa)	P_{yy} (MPa)	P_{ZZ} (MPa)	$P_{correction}$ (MPa)	Total System Pressure (MPa)	Interfacial Tension (mN/m)	Density (Kg/m^3)
10	-13.37	-12.87	-1.31	-1.31	-0.01	62.30	1.64
100	-12.79	-12.88	-0.62	-1.39	0.77	64.46	17.04
512	-7.72	-7.30	2.02	-1.80	3.81	50.26	96.89
1024	-2.95	-3.43	3.90	-2.38	6.28	37.40	213.54
1500	-4.10	-4.18	2.57	-2.99	5.56	35.40	540.53
1700	-3.05	-2.28	3.62	-3.27	6.89	33.17	686.97
2048	9.25	9.08	15.28	-3.78	19.07	32.28	886.47

Table D 4: Results of fourth simulation run using the CO_2-water model at 300K.

RUN4	Pressure Tensors						
No: of CO_2 molecules used	P_{XX} (MPa)	P_{yy} (MPa)	P_{ZZ} (MPa)	$P_{correction}$ (MPa)	Total System Pressure (MPa)	Interfacial Tension (mN/m)	Density (Kg/m^3)
10	-13.60	-13.74	-1.36	-1.31	-0.05	64.97	1.91
100	-12.54	-12.96	-0.60	-1.39	0.79	64.12	15.90
512	-8.35	-7.73	2.30	-1.80	4.10	54.56	90.00
1024	-3.43	-3.57	3.94	-2.38	6.32	39.27	219.89
1500	-5.36	-5.56	2.55	-2.99	5.54	42.27	535.52
1700	-3.30	-4.18	2.45	-3.27	5.72	32.63	704.37
2048	9.00	8.36	15.41	-3.78	19.19	35.52	890.29

Table D 5: Results of fifth simulation run using the CO_2-water model at 300K.

RUN5	Pressure Tensors						
No: of CO_2 molecules used	P_{XX} (MPa)	P_{yy} (MPa)	P_{ZZ} (MPa)	$P_{correction}$ (MPa)	Total System Pressure (MPa)	Interfacial Tension (mN/m)	Density (Kg/m^3)
10	-13.56	-13.62	-1.33	-1.31	-0.03	64.68	2.11
100	-12.41	-12.09	-0.54	-1.39	0.85	61.83	16.79
512	-8.06	-8.13	2.14	-1.80	3.94	54.03	89.63
1024	-3.84	-4.32	3.75	-2.38	6.13	41.34	215.64
1500	-4.53	-5.45	2.82	-2.99	5.81	41.19	547.51
1700	-3.94	-3.84	4.09	-3.27	7.36	42.10	694.17
2048	9.23	9.29	16.44	-3.78	20.22	37.91	884.94

Table D 6: Average values calculated over five simulation runs of the CO_2-water model at 300K.

	Total System Pressure		Interfacial Tension		Bulk CO_2 Density	
No:of CO_2 molecules used	Average Pressure, P_{CO2}(MPa)	Error bar (±)	Average (mN/m)	Error bar (±)	Average (kg/m^3)	Error bar (±)
10	-0.01	0.03	64.76	1.48	1.78	0.24
100	0.78	0.05	63.25	1.12	16.78	0.70
512	3.97	0.11	51.74	2.41	92.51	5.24
1024	6.36	0.28	39.77	1.78	227.63	17.05
1500	5.73	0.26	40.05	2.71	544.39	6.93
1700	6.92	0.97	35.65	3.86	688.19	15.62
2048	19.76	0.70	34.66	2.52	889.00	3.96

Table D 7: Results of first simulation run using the CO_2-brine model at 300K.

RUN1	Pressure Tensors						
Molarity	P_{XX} (MPa)	P_{yy} (MPa)	P_{ZZ} (MPa)	$P_{correction}$ (MPa)	Total System Pressure (MPa)	Interfacial Tension (mN/m)	± Density (Kg/m^3)
0.17	9.21	9.01	16.16	-3.79	19.94	37.16	890.08
1	4.22	4.31	12.62	-3.81	16.43	44.09	870.69
2.1	2.29	1.82	10.48	-3.83	14.31	44.46	853.45
3.5	1.37	0.36	9.11	-3.85	12.96	43.54	835.31

Table D 8: Results of second simulation run using the CO_2-brine model at 300K.

RUN2	Pressure Tensors						
Molarity	P_{XX} (MPa)	P_{yy} (MPa)	P_{ZZ} (MPa)	$P_{correction}$ (MPa)	Total System Pressure (MPa)	Interfacial Tension (mN/m)	Density (Kg/m^3)
0.17	8.92	9.03	15.57	-3.79	19.36	34.80	884.57
1	5.53	5.56	13.24	-3.81	17.04	40.58	865.55
2.1	3.20	3.12	10.46	-3.83	14.28	38.50	845.93
3.5	0.12	-0.11	8.84	-3.85	12.68	46.60	828.61

Table D 9: Results of third simulation run using the CO_2-brine model at 300K.

RUN3	Pressure Tensors						
Molarity	P_{XX} (MPa)	P_{yy} (MPa)	P_{ZZ} (MPa)	$P_{correction}$ (MPa)	Total System Pressure (MPa)	Interfacial Tension (mN/m)	Density (Kg/m^3)
0.17	8.20	8.71	15.22	-3.79	19.01	35.73	884.43
1	5.05	5.18	11.88	-3.81	15.69	35.68	869.75
2.1	2.71	3.47	10.62	-3.83	14.45	39.72	846.46
3.5	0.56	0.55	9.29	-3.85	13.14	46.08	825.93

Table D 10: Results of fourth simulation run using the CO_2-brine model at 300K.

RUN4	Pressure Tensors						
Molarity	P_{XX} (MPa)	P_{yy} (MPa)	P_{ZZ} (MPa)	$P_{correction}$ (MPa)	Total System Pressure (MPa)	Interfacial Tension (mN/m)	Density (Kg/m^3)
0.17	7.59	7.69	14.63	-3.79	18.41	36.85	884.86
1	5.35	5.59	12.30	-3.81	16.10	36.04	866.49
2.1	3.46	3.14	10.37	-3.83	14.20	37.30	846.05
3.5	0.85	0.47	8.67	-3.85	12.51	42.25	827.24

Table D 11: Results of fifth simulation run using the CO_2-brine model at 300K.

RUN5	Pressure Tensors						
Molarity	P_{XX} (MPa)	P_{yy} (MPa)	P_{ZZ} (MPa)	$P_{correction}$ (MPa)	Total System Pressure (MPa)	Interfacial Tension (mN/m)	Density (Kg/m^3)
0.17	9.34	9.69	16.14	-3.79	19.93	34.97	882.53
1	6.15	6.36	12.70	-3.81	16.51	34.00	867.23
2.1	2.43	2.88	9.99	-3.83	13.82	38.70	846.51
3.5	1.60	1.61	9.85	-3.85	13.69	43.49	830.29

Table D 12: Average values calculated over five simulation runs of the CO_2-brine model at 300K.

	Total System Pressure		Interfacial Tension		Bulk CO_2 Density	
Molarity	Average Pressure, P_{co2}(MPa)	Error bar (±)	Average (mN/m)	Error bar (±)	Average (kg/m^3)	Error bar (±)
0.17	19.18	0.65	35.90	1.07	885.29	2.83
1	16.35	0.50	38.08	4.15	867.94	2.19
2.1	14.21	0.24	39.74	2.78	847.68	3.23
3.5	13.00	0.46	44.39	1.86	829.48	3.64

Table D 13: Results of first simulation run using the CO_2-water model at 343.3K

RUN1-343.3K	Pressure Tensors					
No: of CO_2 molecules used	P_{XX} (MPa)	P_{yy} (MPa)	P_{ZZ} (MPa)	$P_{correction}$ (MPa)	Total System Pressure (MPa)	Interfacial Tension (mN/m)
1024	32.09	30.30	101.87	-23.47	12.70	37.79
1500	101.89	99.25	160.83	-29.51	19.29	32.22
1700	181.35	180.83	243.07	-32.26	27.90	33.14

Table D 14: Results of second simulation run using the CO_2-water model at 343.3K

RUN2-343.3K	Pressure Tensors					
No: of CO_2 molecules used	P_{XX} (MPa)	P_{yy} (MPa)	P_{ZZ} (MPa)	$P_{correction}$ (MPa)	Total System Pressure (MPa)	Interfacial Tension (mN/m)
1024	18.96	17.32	89.40	-23.47	11.44	38.10
1500	104.07	104.84	166.23	-29.51	19.83	33.03
1700	171.47	175.66	237.24	-32.26	27.31	34.04

Table D 15: Results of third simulation run using the CO_2-water model at 343.3K

RUN3-343.3K	Pressure Tensors					
No: of CO_2 molecules used	P_{xx} (MPa)	P_{yy} (MPa)	P_{zz} (MPa)	$P_{correction}$ (MPa)	Total System Pressure (MPa)	Interfacial Tension (mN/m)
1024	28.61	27.08	99.18	-23.47	12.43	38.14
1500	90.73	90.89	154.98	-29.51	18.69	34.31
1700	170.34	174.75	236.35	-32.26	27.22	34.11

Table D 16: Results of fourth simulation run using the CO_2-water model at 343.3K

RUN4-343.3K	Pressure Tensors					
No: of CO_2 molecules used	P_{xx} (MPa)	P_{yy} (MPa)	P_{zz} (MPa)	$P_{correction}$ (MPa)	Total System Pressure (MPa)	Interfacial Tension (mN/m)
1024	25.97	24.86	97.10	-23.47	12.22	38.33
1500	99.70	98.00	166.47	-29.51	19.86	36.15
1700	158.94	161.34	222.00	-32.26	25.76	33.07

Table D 17: Results of fifth simulation run using the CO_2-water model at 343.3K

RUN5-343.3K	Pressure Tensors					
No: of CO_2 molecules used	P_{xx} (MPa)	P_{yy} (MPa)	P_{zz} (MPa)	$P_{correction}$ (MPa)	Total System Pressure (MPa)	Interfacial Tension (mN/m)
1024	26.32	24.38	100.58	-23.47	12.57	40.22
1500	91.38	92.25	155.63	-29.51	18.76	34.12
1700	163.02	161.99	221.62	-32.26	25.72	31.61

Table D 18: Results of first simulation run using the CO_2-water model at 374.3K.

RUN1-374.3K	Pressure Tensors					
No: of CO_2 molecules used	P_{xx} (MPa)	P_{yy} (MPa)	P_{zz} (MPa)	$P_{correction}$ (MPa)	Total System Pressure (MPa)	Interfacial Tension (mN/m)
1024	75.67	84.48	148.43	-23.47	17.42	36.55
1500	237.28	240.86	301.06	-29.51	33.50	33.14
1700	358.55	357.01	415.13	-32.26	45.33	30.66

Table D 19: Results of second simulation run using the CO_2-water model at 374.3K.

RUN2-374.3K	Pressure Tensors					
No: of CO_2 molecules used	P_{XX} (MPa)	P_{yy} (MPa)	P_{ZZ} (MPa)	$P_{correction}$ (MPa)	Total System Pressure (MPa)	Interfacial Tension (mN/m)
1024	92.11	85.71	152.86	-23.47	17.87	34.19
1500	223.24	226.41	282.85	-29.51	31.65	31.02
1700	339.88	344.84	398.08	-32.26	43.60	29.79

Table D 20: Results of third simulation run using the CO_2-water model at 374.3K.

RUN3-374.3K	Pressure Tensors					
No: of CO_2 molecules used	P_{XX} (MPa)	P_{yy} (MPa)	P_{ZZ} (MPa)	$P_{correction}$ (MPa)	Total System Pressure (MPa)	Interfacial Tension (mN/m)
1024	93.00	88.87	156.73	-23.47	18.26	35.18
1500	230.44	225.19	282.57	-29.51	31.62	29.28
1700	337.66	332.89	394.32	-32.26	43.22	31.57

Table D 21: Results of fourth simulation run using the CO_2-water model at 374.3K.

RUN4-374.3K	Pressure Tensors					
No: of CO_2 molecules used	P_{XX} (MPa)	P_{yy} (MPa)	P_{ZZ} (MPa)	$P_{correction}$ (MPa)	Total System Pressure (MPa)	Interfacial Tension (mN/m)
1024	73.84	77.92	146.31	-23.47	17.20	37.66
1500	218.82	218.24	277.05	-29.51	31.06	31.29
1700	334.42	337.59	389.48	-32.26	42.73	28.59

Table D 22: Results of fifth simulation run using the CO_2-water model at 374.3K.

RUN5-374.3K	Pressure Tensors					
No: of CO_2 molecules used	P_{XX} (MPa)	P_{yy} (MPa)	P_{ZZ} (MPa)	$P_{correction}$ (MPa)	Total System Pressure (MPa)	Interfacial Tension (mN/m)
1024	79.40	75.85	147.71	-23.47	17.34	37.47
1500	216.53	214.86	273.16	-29.51	30.67	30.72
1700	341.60	340.11	396.06	-32.26	43.40	29.52

Table D 23: Average values calculated over 5 simulation runs of the CO_2-brine model at 343.3K.

Temperature-343.3K	Total System Pressure		Interfacial Tension	
No:of CO_2 molecules used	Average Pressure, P_{co2}(MPa)	Error bar (±)	Average (mN/m)	Error bar (±)
1024	12.27	0.50	38.52	0.98
1500	19.29	0.56	33.97	1.49
1700	26.78	0.98	33.20	1.01

Table D 24: Average values calculated over 5 simulation runs of the CO_2-brine model at 374.3K.

Temperature-374.3K	Total System Pressure		Interfacial Tension	
No:of CO_2 molecules used	Average Pressure, P_{co2}(MPa)	Error bar (±)	Average (mN/m)	Error bar (±)
1024	17.62	0.44	36.21	1.49
1500	31.7	1.08	31.09	1.39
1700	43.66	0.99	30.03	1.14

Table D 25: Results of first simulation run using the SiO_2-water-CO_2- model at 300K.

run1			
No: of CO_2 molecules used	Pressure on CO_2 phase, P_{CO2}(MPa)	Contact Angle(^{o})	Density (kg/m^3)
500	3.5	54.2	57.0
1000	4.5	58.5	109.8
2000	6.2	65.3	299.9
3000	5.7	73.1	584.7
4000	9	75.6	761.7
4913	21	76.4	896.7

Table D 26: Results of second simulation run using the SiO_2-water-CO_2- model at 300K.

Run2			
No: of CO_2 molecules used	Pressure on CO_2 phase, P_{CO2}(MPa)	Contact Angle(^{o})	Density (kg/m^3)
500	1	52.1	28.48436
1000	3.5	62.9	71.30564
2000	6	74.1	186.1866
3000	5.5	76.3	615.9854
4000	10.8	78.33	754.5529
4913	20.5	82.7	896.0936

Table D 27: Results of third simulation run using the SiO_2-water-CO_2 model at 300K.

Run3			
No: of CO_2 molecules used	Pressure on CO_2 phase, P_{CO2}(MPa)	Contact Angle(^{o})	Density (kg/m^3)
500	1	48.3	26.59491
1000	3.5	61.6	73.86711
2000	6	74.4	184.2433
3000	5.3	77.4	619.9617
4000	11.5	86.25	764.0133
4913	21.2	88.1	900.4549

Table D 28: Results of fourth simulation run using the SiO_2-water-CO_2 model at 300K.

Run4			
No: of CO_2 molecules used	Pressure on CO_2 phase, P_{CO2}(MPa)	Contact Angle(^{o})	Density (kg/m^3)
500	1	43	26.14848
1000	3.5	66.36	70.73239
2000	5.2	76.33	155.9235
3000	5.5	79.9	614.4089
4000	11	82.7	761.7925
4913	20.3	83.7	894.4865

Table D 29: Results of fifth simulation run using the SiO_2-water-CO_2- model at 300K.

Run5			
No: of CO_2 molecules used	Pressure on CO_2 phase, P_{CO2}(MPa)	Contact Angle(^{o})	Density (kg/m^3)
500	1	41.1	26.79332
1000	4	64.6	77.64689
2000	5.5	70.2	174.1225
3000	5.5	83.1	621.4666
4000	11.5	85.7	768.4403
4913	20.5	80.3	899.7025

Table D 30: Average values calculated over 5 simulation runs of the SiO_2-water-CO_2 model at 300K.

	Total System Pressure		Contact Angle		Bulk CO_2 Density	
No:of CO_2 molecules used	Average Pressure, P_{co2}(MPa)	Error bar (±)	Average (^{o})	Error bar (±)	Average (kg/m^3)	Error bar (±)
500	1.00	0.00	46.15	4.98	27.01	1.02
1000	3.63	0.25	63.87	2.07	73.39	3.15
2000	5.68	0.39	73.75	2.56	175.12	13.85
3000	5.45	0.10	79.18	3.64	617.96	3.31
4000	11.20	0.36	83.24	3.64	760.12	5.80
4913	20.63	0.39	83.70	3.26	897.68	2.86

Table D 31: Results of five simulation runs using the SiO_2-water-CO_2 model with 4913 CO_2 molecules at 320K.

Temperature-320K	RUN 1	RUN 2	RUN 3	RUN 4	RUN 5	Average	Error bar (±)
Contact Angle(^{o})	79.10	81.50	83.70	81.50	82.80	82.38	1.08
Density (kg/m^3)	884.37	884.15	886.03	883.65	880.52	883.74	2.01

Table D 32: Results of five simulation runs using the SiO_2-water-CO_2 model with 4913 CO_2 molecules at 350K.

Temperature-350K	RUN 1	RUN 2	RUN 3	RUN 4	RUN 5	Average	Error bar (±)
Contact Angle(^{o})	78.80	80.70	84.10	82.40	75.90	80.78	3.53
Density (kg/m^3)	880.09	873.75	875.29	871.74	875.98	875.37	3.10

Table D 33: Results of first simulation run using the SiO_2-brine-CO_2- model at 300K.

Run1			
No: of CO_2 molecules used-1200 Molarity	Pressure on CO_2 phase, P_{CO2}(MPa)	Contact Angle(^{o})	Density (kg/m^3)
0.17	5	60.6	142.22
1.0	5	61.7	139.86
2.1	5	65.35	133.89
3.5	5	66.9	145.69

Table D 34: Results of second simulation run using the SiO_2-brine-CO_2- model at 300K.

Run2			
No: of CO_2 molecules used-1200 Molarity	Pressure on CO_2 phase, P_{CO2}(MPa)	Contact Angle(^{o})	Density (kg/m^3)
0.17	4	61.9	100.00
1.0	4	68.8	96.61
2.1	4	74.5	97.39
3.5	4	69.5	98.34

Table D 35: Results of third simulation run using the SiO_2-brine-CO_2 model at 300K.

Run3			
No: of CO_2 molecules used-1200 Molarity	Pressure on CO_2 phase, P_{CO2}(MPa)	Contact Angle(^{o})	Density (kg/m^3)
0.17	4	65.1	99.80
1.0	4	69	92.62
2.1	4	72.9	100.27
3.5	4	68.6	93.10

\\

Table D 36: Results of fourth simulation run using the SiO_2-brine-CO_2 model at 300K.

Run4			
No: of CO_2 molecules used-1200 Molarity	Pressure on CO_2 phase, P_{CO2}(MPa)	Contact Angle(^{o})	Density (kg/m^3)
0.17	4	66.1	102.59
1.0	4	70	98.00
2.1	4	73	99.53
3.5	4	71	98.92

Table D 37: Results of fifth simulation run using the SiO_2-brine-CO_2 model at 300K.

Run5			
No: of CO_2 molecules used-1200 Molarity	Pressure on CO_2 phase, P_{CO2}(MPa)	Contact Angle(^{o})	Density (kg/m^3)
0.17	4	65.5	98.10
1.0	4	70	94.88
2.1	4	68.2	97.91
3.5	4	68.2	94.14

Table D 38: Average values calculated over last 4 simulation runs of the SiO_2-brine-CO_2 model at 300K.

No: of CO_2 molecules used-1200 Molarity	Average pressure on CO_2 phase, P_{CO2}(MPa)	Contact Angle(^{o})		Density (kg/m^3)	
		Average	Error bar (±)	Average	Error bar (±)
0.17	4	64.65	1.88	100.12	1.85
1.0	4	69.45	0.64	95.53	2.32
2.1	4	72.15	2.73	98.78	1.35
3.5	4	69.33	1.24	96.13	2.93

Table D 39: Results of simulation at 300K of SiO_2-brine-CO_2 model with higher interaction between quartz and NaCl (3.5M)

	Contact angle (^{o})	Density (kg/m^3)
run1	42.8	115.32
run2	45.6	104.3091
run3	51.2	102.4017
run4	52.3	102.9927
run5	48.4	103.3704
average (last 4 runs)	49.375	103.2685
error bar (±)	3.00485718	0.800142

APPENDIX E Simulated Images of Water Droplet Under Various Thermodynamic Conditions.

(NOTE: In all the simulated images shown below, the green curve represents the isodensity lines drawn for the calculation of contact angles and the red curve represents the water droplet.)

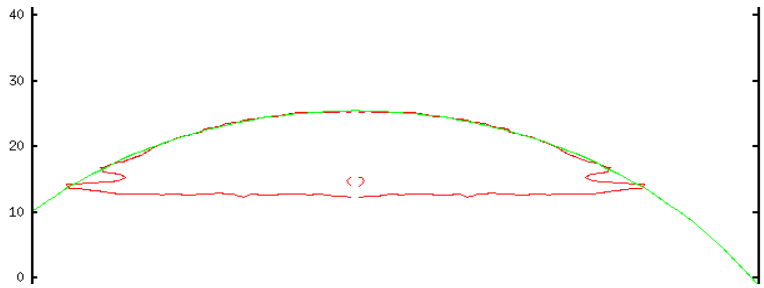

Figure E 1: Simulated image of water droplet under a CO_2 density of 26.79Kg/m^3 at 300K.

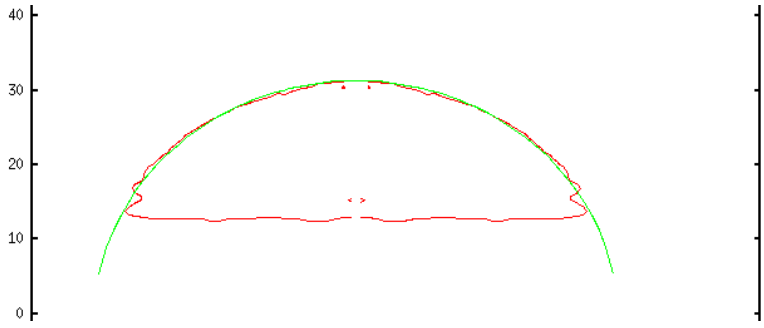

Figure E 2: Simulated image of water droplet under a CO_2 density of 77.65Kg/m^3 at 300K.

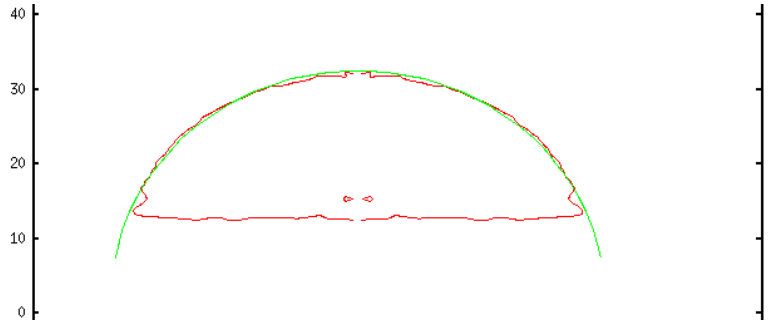

Figure E 3: Simulated image of water droplet under a CO_2 density of 174.12Kg/m^3 at 300K.

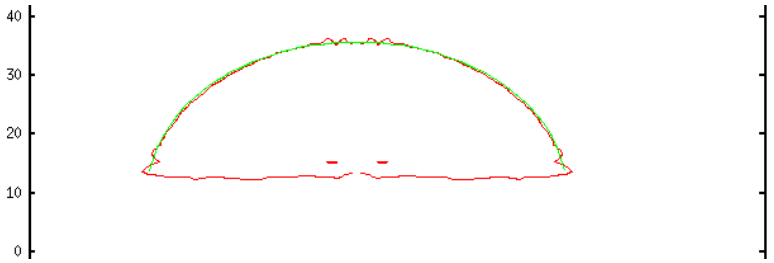

Figure E 4: Simulated image of water droplet under a CO_2 density of 621.47Kg/m^3 at 300K.

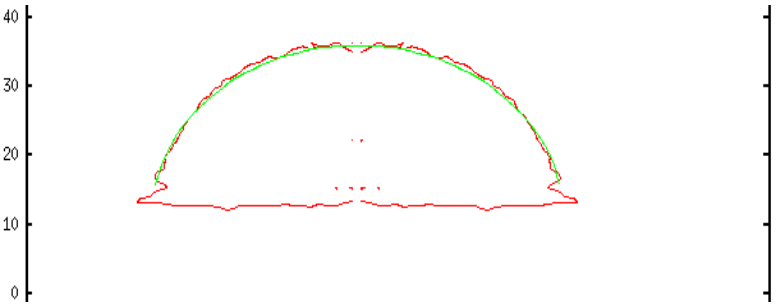

Figure E 5: Simulated image of water droplet under a CO_2 density of 768.44Kg/m^3 at 300K.

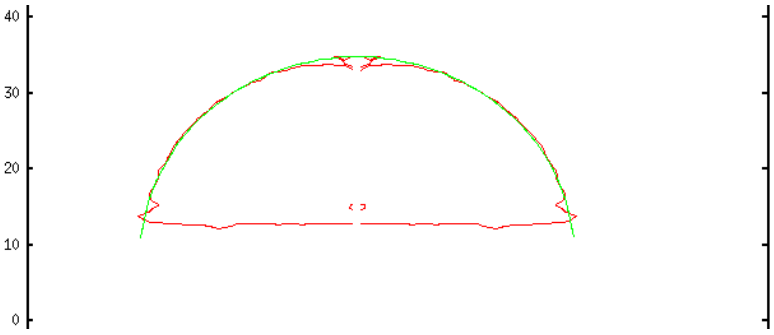

Figure E 6: Simulated image of water droplet under a CO_2 density of 899.7Kg/m^3 at 300K.

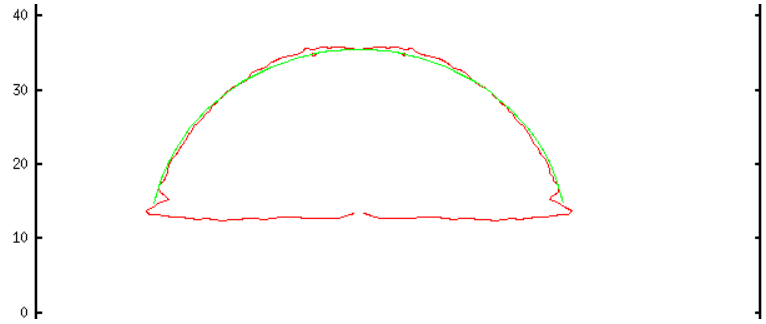

Figure E 7: Simulated image of water droplet under a CO_2 density of 880.52Kg/m^3 at 320K.

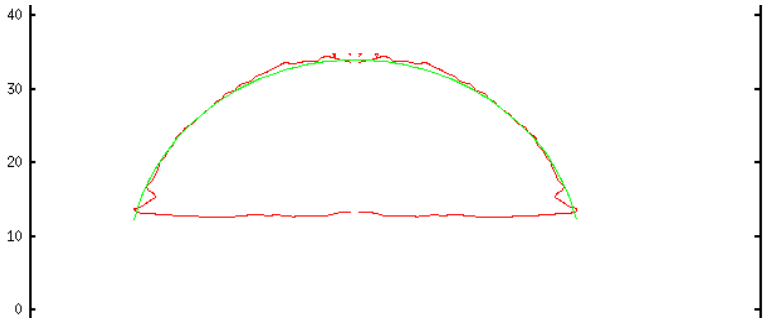

Figure E 8: Simulated image of water droplet under a CO_2 density of 875.98Kg/m^3 at 350K.

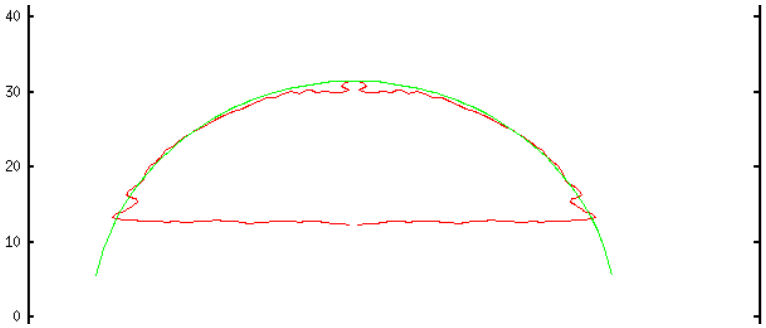

Figure E 9: Simulated image of water droplet at 300K under a CO_2 pressure (P_{CO2}) of 4MPa and 0.17M.

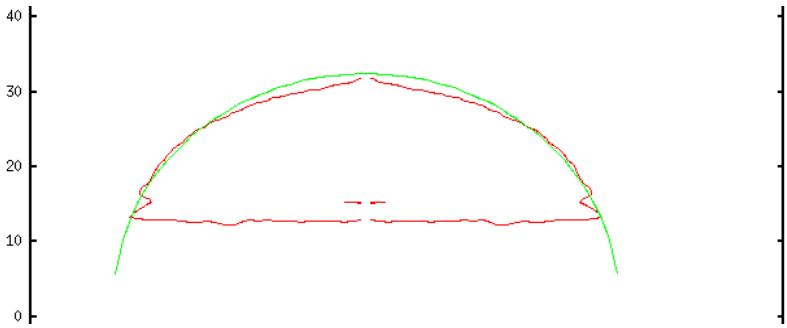

Figure E 10: Simulated image of water droplet at 300K under a CO_2 pressure (P_{CO2}) of 4MPa and 1M NaCl.

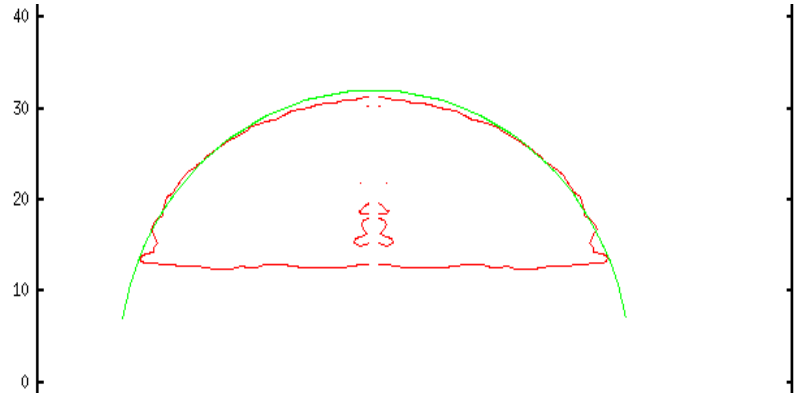

Figure E 11: Simulated image of water droplet at 300K under a CO_2 pressure (P_{CO2}) of 4MPa and 2.1M NaCl.

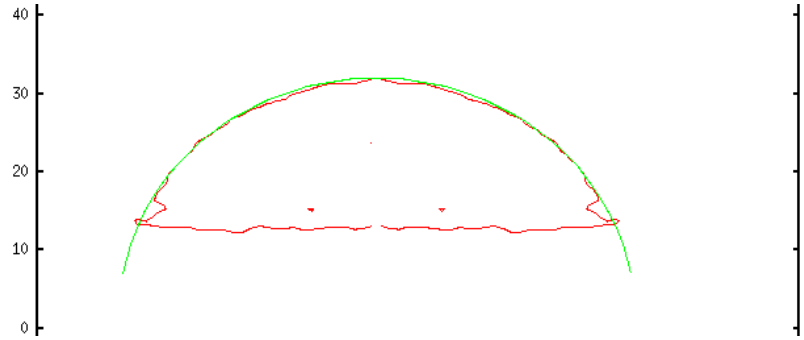

Figure E 12: Simulated image of water droplet at 300K under a CO_2 pressure (P_{CO2}) of 4MPa and 3.5M NaCl.

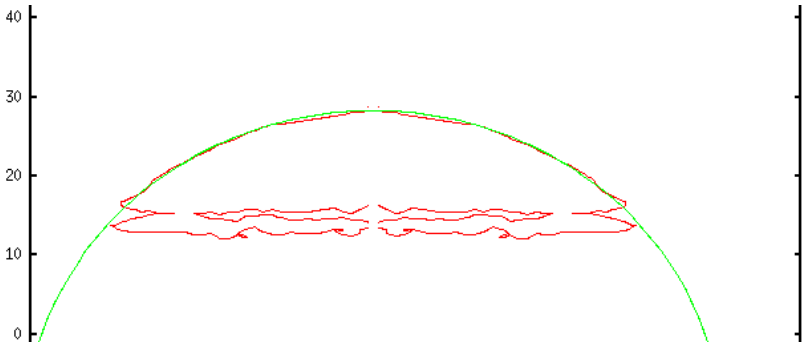

Figure E 13: Simulated image of water droplet at 300K under a CO_2 pressure (P_{CO2}) of 4MPa and 3.5M NaCl with higher interaction between quartz and NaCl.

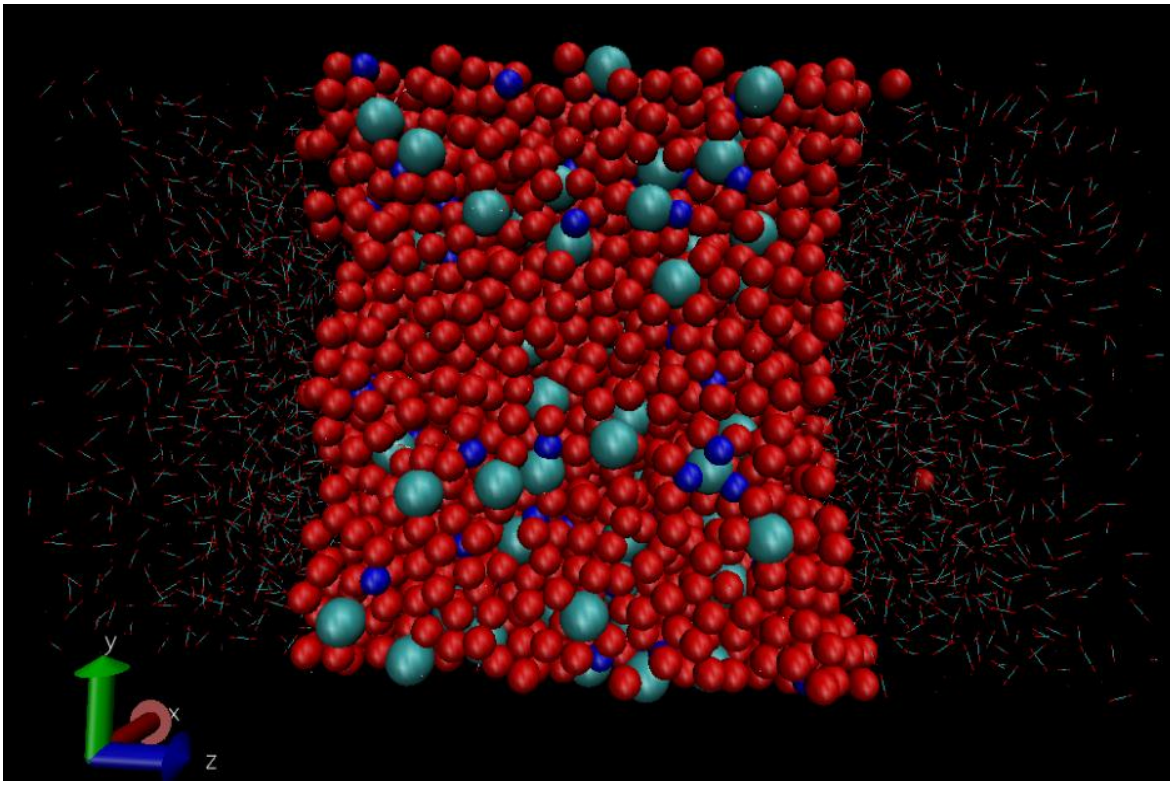

Figure E 14: 3-dimensional view of the final configuration of CO_2-brine system after simulation (red spheres-water, light and dark blue- NaCl and thin particles surrounding are CO_2).